University of Thessaly, School of Engineering, Department of Mechanical Engineering

Air flow optimization through an intake system for a four-cylinder Formula Student (FSAE) racecar.

Integrated Master of Science Thesis
Academic Advisor: Dr. Nikos Pelekasis

Aglaia Schiza
25/2/2020

Submitted in Partial Fulfillment

of the requirements for the degree

of Integrated Master in Mechanical Engineering

Certified by the members of the Thesis Committee

First Examiner   Prof. Nikos Pelekasis

(Academic Advisor)   Professor of Computational Fluid Dynamics, University of Thessaly

Second Examiner   Prof. Stamatelos Tassos

Professor of Internal Combustion Engines, University of Thessaly

Third Examiner   Prof. Charalampous Georgios

Professor Thermofluid Processes with Energy Applications, University of Thessaly

ABSTRACT

Intake tuning and ram effect are widely known methods to increase engine performance. This thesis details the design, study and results of an intake system implemented on a Honda CBR 600RR 2007 engine, equipped with a restrictor downstream the throttle body, in accordance with the Formula SAE competition rules. With the use of the calculation formulas of the tuning theory and the one-dimensional simulations of the engine at Ricardo Wave, the length and the diameters of the intake ducts and beyond the plenum volume were defined so as to obtain the maximum torque possible in the range of 6000 to 12000 rpm. After the dimensioning process, the assembly was modeled in CAD, analyzing the packaging requirements determined by the regulations and a better adaptation of the system to the prototype and simulated with the aid of Ansa pre-processor and Ansys Fluent simulation package. The combination of the packaging restrictions with the pressure distribution and velocity streamlines led to the final design of the intake system. Finally, the air intake was fabricated with the use of aluminum and implemented on the racecar. As the general concept of the Formula SAE competitions demands, extensive testing of the system was conducted on the dynamometer and on track so as its smooth and effective operation with rest of the racecar's subsystems is ensured.

ACKNOWLEDGEMENT

First of all, I would like to thank my thesis advisor Dr. Nikos Pelekasis, of the department of Mechanical Engineering, at the University of Thessaly. He gave me the opportunity to develop a theme that I have always found more than interesting, a theme that may define my future someday.

I would also like to warmly thank the Formula Student team of the University of Thessaly, Centaurus Racing Team, in which I was a member for three years. My participation in the team cultivated my engineering mentality, introduced me to the real-life working environment and gave me sentiments that I will always remember with joy.

Finally, I cannot but to express my profound gratitude to my parents,my whole family and friends for providing me with support and encouragement throughout all my years of study. The accomplishment of this thesis and the forthcoming acquisition of my degree would not have been possible without them. Thank you.

Author,

Schiza Aglaia

TABLE OF CONTENTS

TABLE OF EQUATIONS

TABLE OF FIGURES

1. INTRODUCTION

1.1 FSAE Competition

Formula Student is a student engineering competition held annually in various countries. Students build a single seat formula racecar with which they can compete against teams from all over the world. The competition is not won solely by the team with the fastest car, but rather by the team with the best overall package of construction, performance, and financial and sales planning.

Formula Student challenges the team members to go the extra step in their education by incorporating into it intensive experience in building and manufacturing as well as considering the economic aspects of the automotive industry. Teams take on the assumption that they are a manufacturer developing a prototype to be evaluated for production. The target audience is the non-professional Weekend-Racer. The racecar must show very good driving characteristics such as acceleration, braking and handling. It should be offered at a very reasonable cost and be reliable and dependable. Additionally, the car's market value increases through other factors such as aesthetics, comfort and the use of readily available, standard purchase components.

The challenge the teams face is to compose a complete package consisting of a well constructed racecar and a sales plan that best matches these given criteria. The decision is made by a jury of experts from the motorsport, automotive and supplier industries. The jury will judge every team's car and sales plan based on construction, cost planning and sales presentation. The rest of the judging will be done out on the track, where the students demonstrate in a number of performance tests how well their self-built racecars fare in their true environment.

1.2 Engine Performance

The preparation of an internal combustion engine relies on several parameters of its operation. Having this considered, many are the development fields to be considered in order to obtain maximum performance. The air intake and fuel-air mixture creation are fundamental steps to reach this goal. The intake collector is the component responsible for guaranteeing the connection between the throttle body, responsible for the air intake control, and the engine cylinder head. The collector, constituted by a set of ducts interconnected by an intermediary chamber, has as main goal the delivery of the air-fuel mixture to the intake ports.

Engines that power prototypes of the Formula SAE category must go through alterations on the intake system, being this necessary to comply with the competition rules. The diameter restriction of 20 mm downstream of the throttle body causes a severe diminishment of the system's mass flow and, therefore, the same happens to its indicated power. A method known to improve the engine's performance in these conditions is the intake system tuning which allows improvements at low costs without the use of superchargers or turbochargers. The main goal of this work is an intake system design for the Centaurus Racing Team's prototype,Thireus, by conducting proper dimensioning of the restrictor, intake runners and plenum volume through numerical simulations at Ansys fluent.

1.3 Computational Fluid Dynamics

In simple terms, the simulation tool, ANSYS fluent in my case, is a black box. The user provides the software with inputs, typically geometry, mesh, boundary conditions and material properties and gets the results. However, the importance of knowing what processes are being held under the black box is significant so as to ensure that the final results are accurate and as close to the reality as possible.

In order to proceed with what is underlying the black box, the first step followed is the understanding of the physical model that has to be solved. However, fluent is only able to solve a mathematical model of the physical problem that is based on some key physical principles and assumptions as well.

After that, with the proper use of numerical methods a numerical solution for selected variables is obtained. In a CFD case, these variables can be pressure or velocity, for example. The aforementioned variables are calculated in specific points, which are defined by the mesh generation.

Everything else in the solution field, such as the contour plots, is constructed from those selected variables at the selected points through a process called post-processing.
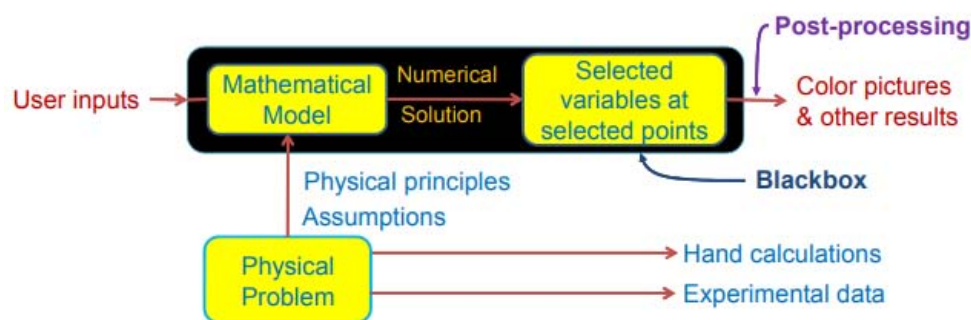
Figure 1 - CFD process diagram

The theory in which this work relies upon, as well as its design methodology, simulations, manufacturing processes and results are to be presented on the following items.

2.LITERATURE REVIEW

2.1 Engine Performance

One of the parameters determining the engine's performance is the torque obtained and it is of extreme importance to know what factors this property arises from. The torque may be described through the following equation:

$$T = \frac{\eta_f \eta_v Q_{HV} \rho_{a,i} (F/A) V_d}{4\pi}$$

Equation 1

In light of the aforementioned, the importance of the volumetric efficiency in the engine's performance shall be verified. This one (the volumetric efficiency) can be described by the following equation 2:

$$\eta_v = \frac{2\dot{m}_a}{\rho_{a,i} V_d N}$$

Equation 2

The volumetric efficiency is affected by various variables in the engine's operation, such as the design of the intake and exhaust headers and ports, the temperature of the incoming mixture and the ratio of pressures at the intake and exhaust systems. Therefore, the intake system shall enhance the most the volumetric efficiency. In order to accomplish this, design criteria that come to be important are: a low air flow resistance, an even distribution of air and fuel among the cylinders, sufficient, but not excessive, heating in order to guarantee the correct fuel vaporization, and proper duct length in order to obtain the most out of the ram and tuning effects.

2.2 Intake System Restrictor

2.2.1 Restrictions and Regulations

According to the FSAE rules regarding the air intake system "IC1.6.1 In order to limit the power capability from the engine, a single circular restrictor must be placed in the intake system and all engine airflow must pass through the restrictor. The only allowed sequence of components are the following:

a. For naturally aspirated engines, the sequence must be (see Fig 1): throttle body, restrictor, and engine"

b. For turbocharged or supercharged engines, the sequence must be (see Fig 2): restrictor, compressor, throttle body, engine.
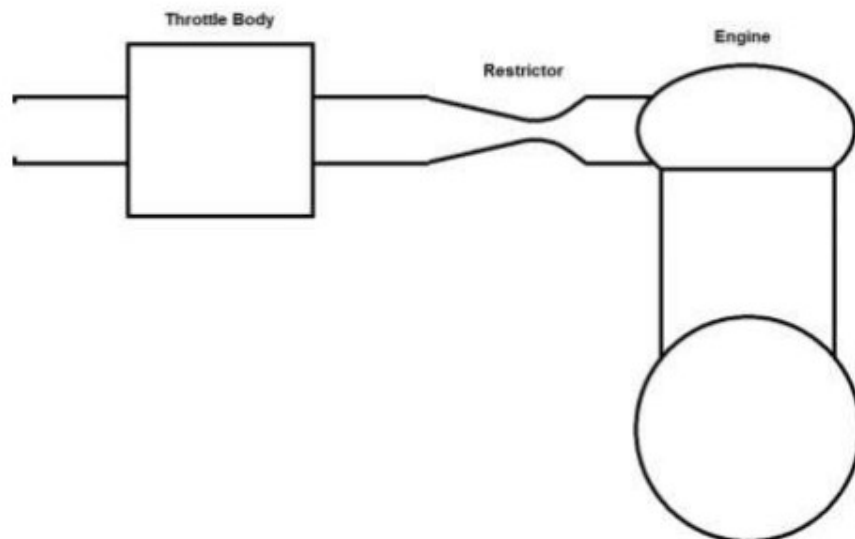
Figure 2 - Restrictor FSAE rules for naturally aspirated engines
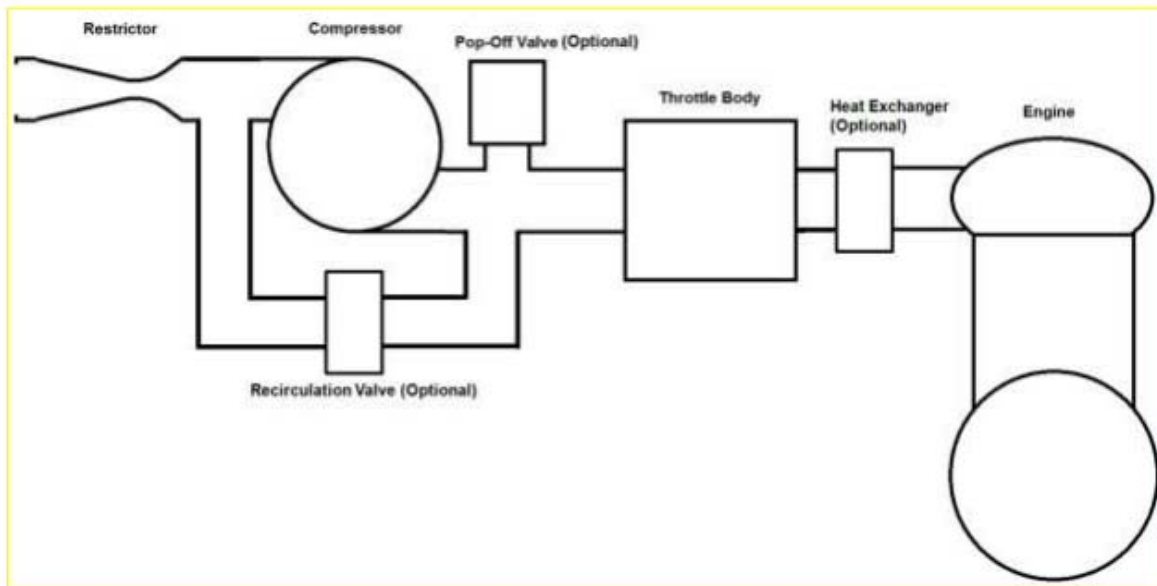
Figure 3 - Restrictor FSAE rules for supercharged engines

IC1.6.2 The maximum restrictor diameters at any time during the competition are:

a. Gasoline fueled cars - 20.0 mm (0.7874 inch)
b. E-85 fueled cars – 19.0 mm (0.7480 inch)

IC1.6.3 The restrictor must be located to facilitate measurement during the inspection process.

IC1.6.4 The circular restricting cross section may not be movable or flexible in any way, e.g. the restrictor may not be part of the movable portion of a barrel throttle body.

IC1.6.5 If more than one engine is used, the intake air for all engines must pass through the one restrictor.

For the aforementioned reasons, the restrictor has to be designed in a way that provides the system with the maximum possible mass flow rate but with the minimum pull from the engine. Additionally, the pressure inside the restrictor has to be recovered at the minimum length. Finally, its' position should allow as cold air as possible to come through, in order to take advantage of its' high density and finally achieve higher volumetric efficiency. All the above, have to be combined in an efficient packaging.

2.2.2 Placement

The horsepower output of the engine is linearly related with the density of air that is pulled into the cylinder. The higher the density of the air that sucks into the cylinder, more fuel will be able to combust during the working cycle, fact that increases the force applied on the piston and as a consequence higher torque output is achieved. According to the ideal gas law:

Pv = RT, v=1/ρ→P=ρRT   **Equation 3**

Based on this relationship, we concluded that in order to maximize the horsepower output of our engine, we needed to shape the geometry of the air intake in such a way as to allow the maximum flow of the coolest air. That's for the restrictor has been placed above driver's helmet. At this position we can also take advantage of the car's velocity, so as to reach greater dynamic pressure at the inlet. Indicative for a car velocity of 80 km/h or 100 km/h the inlet pressure will be:

- 101325+0.5∗1∗222=101567 Pa
- 101325+0.5∗1∗2772=101709 Pa, respectively.

The above mentioned pressure difference helps to achieve greater mass flow rate because leads to chocked flow, unlike to the difference of 101325-90000 = 11325 Pa which gives a Mach number of 0.85.

2.2.3 Shape

The shape of a restrictor can be as simple as a plate with the mandated dimensions machined into it. An orifice plate is a thin plate with a hole in the middle. It is usually placed in a pipe in which fluid flows. When the fluid reaches the orifice plate, the fluid is forced to converge to go through the small hole; the point of maximum convergence actually occurs shortly downstream of the physical orifice, at the so-called vena contracta point. As it does so, the velocity and the pressure change. Beyond the vena contracta, the fluid expands and the velocity and pressure change once again.However, a simple orifice plate would create a lot of pressure loss downstream of the restrictor, and as a result, increased inefficiency.

Instead of placing a simple orifice plate, a venturi-shaped restrictor was chosen: The air's velocity increases as it passes through a constriction in accordance with the principle of mass continuity while its static pressure decreases following the principle of conservation of mechanical energy. Thus any gain in kinetic energy a fluid may accrue due to its increased velocity through a constriction is balanced by a drop in pressure.

2.3 Plenum

The plenum area is where the intake runners meet. At first, the capacity of the plenum had to be decided. A relatively large plenum favors the horsepower, because of the provided air availability at any time. On the other side, a very large plenum can cause problems in throttle response due to the inertia of the static air, when the throttle pedal is pushed, fact that can be tested only on the track. For unrestricted engines the ideal plenum volume is two to 4 and a half times the displacement and for restricted almost reaches the four liters. For my case, the golden section of the volume and the throttle response was found to be the three-liter plenum.

As for the shape, a fully symmetrical geometry with smooth curves was chosen so as to achieve good flow distribution in the four cylinders and minimize losses. However, due to the financial conditions of the team the construction of the intake system had to be implemented using aluminum as a material. Therefore, its shape had to be constricted and not any kind of curvature could be applied.

A steady state fluid model was set in order to test the flow uniformity inside the whole intake system. Although the flow inside is inherently unsteady, the same steady state model used for the restrictor's study was preferred so as to decide the general intake system geometrical characteristics and reduce the computational time requirements.

2.4 Runners

When an engine is running, there are high and low pressure waves moving in the manifold caused by the inertia of the air and the opening and closing of the valves. The idea of port tuning is to have a high pressure wave approach the intake valve before it closes or just as it opens, forcing in a little more intake charge.

On the intake stroke, the piston makes a negative pressure wave that travels from the piston to the intake tract. Once that negative pressure wave reaches the plenum area, it is reflected as a positive pressure wave. That positive pressure wave travels back towards the cylinder. If it reaches the intake valve just before it closes, it will force a little more air in the cylinder. The second, less realized, cause of pressure wave is the exhaust. If a well-functioning exhaust system that scavenges well is implemented, during the overlap period there will be an negative pressure wave as the exhaust is scavenging and pulling in fresh intake charge. The same phenomenon happens, it travels up the intake and is reflected at the plenum area as a positive pressure wave. If the length is correct for the rpm range, the positive pressure will be at the valve just prior to its closing and aid the better repletion of the cylinder. The third and most complex cause of pressure waves is when the intake valve closes, any velocity left in the intake port column of air will make high pressure at the back of the valve. This high pressure wave travels towards the open end of the intake

tract and is reflected and inverted as a low pressure wave. When this low pressure wave reaches the intake valve, it is closed and the negative wave is reflected (it is not inverted due to the valve being closed), once again it reaches the open end of the intake tract and is inverted and reflected back toward the intake valve. This time the valve should just be opening if the port is tuned to the rpm range and the high pressure wave can help force inside the cylinder an additional portion of air.

2.5 CFD model

The final setup found to be the optimum choice for the CFD simulations of the air intake system is the following one:

1) Pressure based solver
2) Energy equation
3) K-omega SST equations
4) Material: Ideal gas
5) Operating conditions
   - 0 atm
   - 300 K
6) Solution methods
   - Coupled scheme
   - Gradient → Least squares cell based
   - Pressure → Second Order
   - Density Momentum → Second Order Upwind
   - Turbulent Kinetic Energy → Second Order Upwind
   - Specific Dissipation Rate → Second Order Upwind
   - Energy → Second Order Upwind
7) Solution Initialization → Hybrid Initialization

Boundary Conditions
   - Pressure Inlet: 101325 Pa
   - Pressure Outlet: 90000 Pa

All the above chosen parameters which conduced to the final solution are explained in detail below.

2.5.1 Compressible Flows

Compressibility effects are encountered in gas flows at high velocity and/or in which there are large pressure variations. When the flow velocity approaches or exceeds the speed of sound of the gas or when the pressure change in the system ($\Delta p/p$) is large, the variation of the gas density with pressure has a significant impact on the flow velocity, pressure, and temperature.

When to Use the Compressible Flow Model

Compressible flows can be characterized by the value of the Mach number:

$$M \equiv u/c$$

<div align="center">

Equation 4

</div>

Here, c is the speed of sound in the gas:

$$c = \sqrt{\gamma RT}$$

<div align="center">

Equation 5

</div>

and **γ** is the ratio of specific heats (cp/cv).

When the Mach number is less than 1.0, the flow is termed subsonic. At Mach numbers much less than 1.0, compressibility effects are negligible and the variation of the gas density with pressure can safely be ignored in the flow modeling. As the Mach number approaches 1.0 (transonic flow regime), compressibility effects become important. When the Mach number exceeds 1.0, the flow is termed supersonic, and may contain shocks and expansion fans which can impact the flow pattern significantly.

Physics of Compressible Flows

Compressible flows are typically characterized by the total pressure **Po** and total temperature **To** of the flow. For an ideal gas, these quantities can be related to the static pressure and temperature by the following:

$$\frac{p_0}{p} = exp(\frac{\int_T^{T_0} \frac{C_p}{T}dT}{R})$$

<div align="center">

Equation 6

</div>

For constant Cp, the previous equation reduces to:

$$\frac{p_0}{p} = \left(1 + \frac{\gamma - 1}{2}M^2\right)^{\gamma/(\gamma-1)}$$

$$\frac{T_0}{T} = 1 + \frac{\gamma - 1}{2}M^2$$

These relationships describe the variation of the static pressure and temperature in the flow as the velocity changes under isentropic conditions. For example, given a pressure ratio from inlet to exit (total to static), Equation (7) can be used to estimate the exit Mach number which would exist in a one-dimensional isentropic flow. For air, Equation (7) predicts a choked flow (Mach number of 1.0) at an isentropic pressure ratio, p/p0, of 0.5283. This choked flow condition will be established at the point of minimum flow area (e.g., in the throat of a nozzle). In the subsequent area expansion of the flow may either accelerate to a supersonic flow in which the pressure will continue to drop, or return to subsonic flow conditions, decelerating with a pressure rise. If a supersonic flow is exposed to an imposed pressure increase, a shock will occur, with a sudden pressure rise and deceleration accomplished across the shock.

Basic Equations for Compressible Flows

Compressible flows are described by the standard continuity and momentum equations solved by ANSYS FLUENT. The energy equation solved by ANSYS FLUENT correctly incorporates the coupling between the flow velocity and the static temperature, and should be activated whenever a compressible flow is being solved. In addition, due to the use of the pressure-based solver, the viscous dissipation terms which become important in high-Mach-number flows should be activated.

The Compressible Form of the Gas Law

For compressible flows, the ideal gas law is written in the following form:

$$\rho = \frac{p_{op} + p}{\frac{R}{M_w}T}$$

where p_{op} is the operating pressure, p is the local static pressure relative to the operating pressure, R is the universal gas constant, and M_w is the molecular weight. The temperature, T, will be computed from the energy equation.

19

Modeling Inputs for Compressible Flows

To set up a compressible flow in ANSYS FLUENT, the following steps were followed:

1. Setup of the **Operating Pressure**:

    - **Boundary Conditions** --> **Operating Conditions**

p_{op} is the absolute static pressure at a point in the flow where the gauge pressure p was defined to be zero.

2. Activation of the solution of the energy equation.

    - **Models** --> **Energy** --> **Edit**

3. For the turbulent flow modelling using pressure-based solver, the optional viscous dissipation terms were activated in the energy equation by turning on Viscous Heating.

    - **Models** --> **Viscous** --> **Edit**

4. Concerning the materials, the ideal-gas option was chosen and all the relevant properties (specific heat, molecular weight, thermal conductivity, etc.) were defined.

5. Continuing, the cell zone conditions and boundary conditions were set ensuring the choice of a well-posed cell zone or boundary condition combination that is appropriate for the flow regime.

2.5.2 Boundary Conditions

Well-posed inlet and exit boundary conditions for compressible flows are considered the following:

- For flow inlets:

    - Pressure inlet: Inlet total temperature and total pressure and, for supersonic inlets, static pressure
    - Mass flow inlet: Inlet mass flow and total temperature
- For flow exits:
    - Pressure outlet: Exit static pressure.

.

2.5.3 Using the Solver

Pressure-Velocity Coupling Method

ANSYS FLUENT provides four segregated types of algorithms: SIMPLE, SIMPLEC, PISO, and (for time-dependant flows using the Non-Iterative Time Advancement option (NITA)) Fractional Step (FSM). These schemes are referred to as the pressure-based segregated algorithm. Steady-state calculations will generally use SIMPLE or SIMPLEC, while PISO is recommended for transient calculations. PISO may also be useful for steady-state and transient calculations on highly skewed meshes. In ANSYS FLUENT, using the Coupled algorithm enables full pressure-velocity coupling, hence it is referred to as the pressure-based coupled algorithm.

Selecting Coupled from the Pressure-Velocity Coupling drop-down list indicates the use of the pressure-based coupled algorithm. This solver offers some advantages over the pressure-based segregated algorithm. The pressure-based coupled algorithm obtains a more robust and efficient single phase implementation for steady-state flows. It is not available for cases using the Eulerian multiphase, NITA, and periodic mass-flow boundary conditions

Setting Under-Relaxation Factors

The pressure-based solver uses under-relaxation of equations to control the update of computed variables at each iteration. This means that all equations solved using the pressure-based solver, will have under-relaxation factors associated with them.

Becauce the Coupled algorithmis chosen in this specific case, the Courant number has to be specified and set at 200 by default, as well as the Explicit Relaxation Factors for Momentum and Pressure, which are set at 0.75 by default.

Initializing the Solution

Before starting the CFD simulation, ANSYS FLUENT must be provided with an initial guess for the solution flow field.

There are two methods for initializing the solution:

- Initialization of the entire flow field in all cells, which is the option used for the intake system simulation and,
- patch values or functions for selected flow variables in selected cell zones or "registers'' of cells. Registers are created with the same functions that are used to mark cells for adaption.

2.5.4 Modeling Turbulence

Turbulent flows are characterized by fluctuating velocity fields. These fluctuations mix transported quantities such as momentum, energy, and species concentration, and cause the transported quantities to fluctuate as well. Since these fluctuations can be of small scale and high frequency, they are too computationally expensive to simulate directly in practical engineering calculations. Instead, the instantaneous governing equations can be time-averaged, ensemble-averaged, or otherwise manipulated to remove the resolution of small scales, resulting in a modified set of equations that are computationally less expensive to solve. However, the modified equations contain additional unknown variables, and turbulence models are needed to determine these variables in terms of known quantities.

In my case study, the characteristic Reynolds number had to be calculated in order to understand if the flow inside the intake system is turbulent or laminar.

$$\mathrm{Re}_L = \frac{\rho U L}{\mu}$$
$$L = x, d, d_h, \text{etc.}$$

Equation 10

As can be seen in the calculations of the flow inside the air intake system that are presented in the next chapter the flow was found to be turbulent so it was modelled accordingly. A descriptive depiction of the turbulent flow structure can be seen in the following figure:
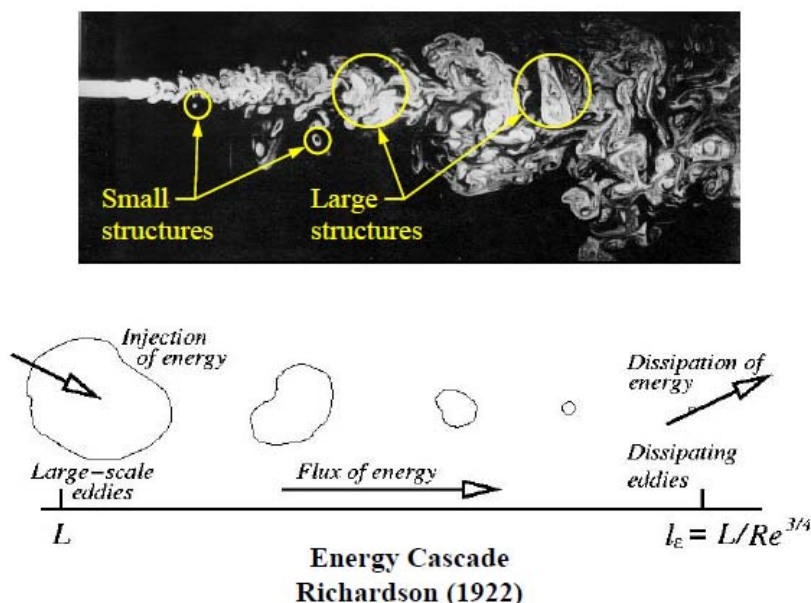

Figure 4 - Turbulent flow structure

There are three different approaches which can be used so as the ''turbulent flow'' problem can be solved.

The first category of models is the Reynolds-Averaged Navier-Stokes (RANS) which solve ensemble-averaged (or time-averaged) Navier-Stokes equations. It is the most widely used approach for calculating industrial flows and all the turbulent length scales are modeled in RANS.

The second one is the Large Eddy Simulation (LES) which solves the spatially averaged Navier-Stokes equations. Large eddies are directly resolved, but eddies smaller than the mesh are modeled. It is a less expensive method than the Direct Numerical Simulation but the amount of computational resources and efforts are still too large for most practical applications.

Finally, all turbulent flows, theoretically, can be simulated by numerically solving the full Navier-Stokes equations which means that the whole spectrum of scales is resolved and no modeling is required. However, the cost is too prohibitive and it constitutes a method not practical for industrial flows. Additionally, it is not available in Fluent.

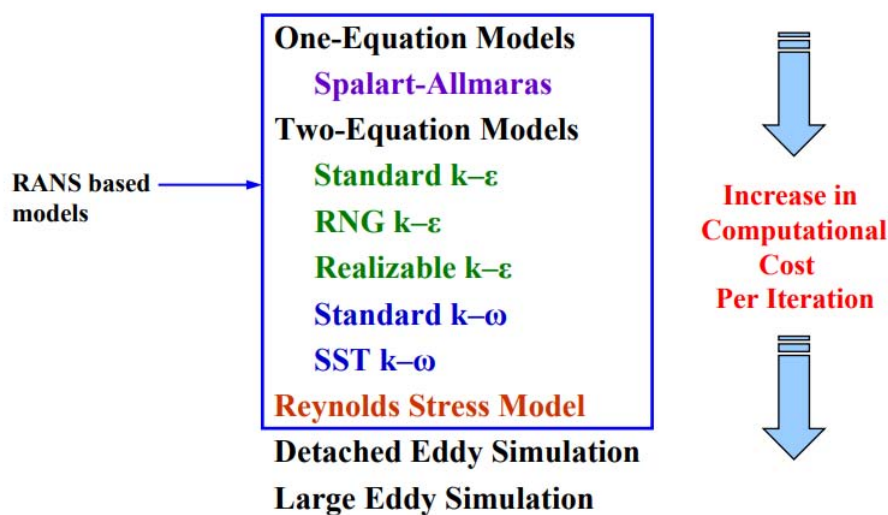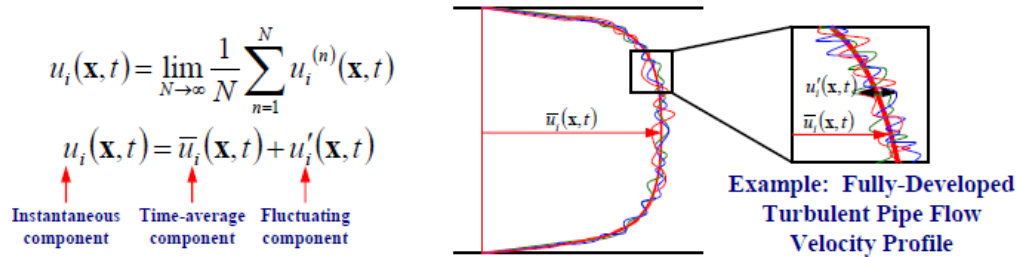The turbulence models available in Fluent are the following:

Figure 5 - Turbulent models available in ANSYS fluent

For RANS modeling ensemble averaging may be used to extract the mean flow properties from the instantaneous ones:

$$u_i(\mathbf{x},t) = \lim_{N\to\infty} \frac{1}{N} \sum_{n=1}^{N} u_i^{(n)}(\mathbf{x},t)$$

$$u_i(\mathbf{x},t) = \overline{u}_i(\mathbf{x},t) + u_i'(\mathbf{x},t)$$

Instantaneous component   Time-average component   Fluctuating component

Example: Fully-Developed Turbulent Pipe Flow Velocity Profile

Equation 11

The Reynolds-averaged momentum equations are as follows:

$$\rho\left(\frac{\partial \overline{u}_i}{\partial t} + \overline{u}_k \frac{\partial \overline{u}_i}{\partial x_k}\right) = -\frac{\partial \overline{p}}{\partial x_i} + \frac{\partial}{\partial x_j}\left(\mu \frac{\partial \overline{u}_i}{\partial x_j}\right) + \frac{\partial R_{ij}}{\partial x_j} \qquad R_{ij} = -\rho\overline{u_i'u_j'}$$

(Reynolds stress tensor)

Equation 12

The Reynolds stresses are additional unknowns introduced by the averaging procedure, hence they must be modeled (related to the averaged flow quantities) in order to close the system of governing equations.

The RANS models can be closed in one of the following ways:

- Eddy Viscosity Models (via the Boussinesq hypothesis)

$$R_{ij} = -\rho\overline{u_i'u_j'} = \mu_T\left(\frac{\partial \overline{u}_i}{\partial x_j} + \frac{\partial \overline{u}_j}{\partial x_i}\right) - \frac{2}{3}\mu_T \frac{\partial \overline{u}_k}{\partial x_k}\delta_{ij} - \frac{2}{3}\rho k \delta_{ij}$$

Equation 13

The Boussinesq hypothesisclaims that the Reynolds stresses are modeled using an eddy (or turbulent) viscosity, μ_T. The hypothesis is reasonable for simple turbulent shear flows: boundary layers, round jets, mixing layers, channel flows, etc.

- Reynolds-Stress Models

These models are implemented via transport equations for Reynolds stresses. Modeling is still required for many terms in the transport equations.RSM is more advantageous in complex 3D turbulent flows with large streamline curvature and swirl, but the model is more complex, computationally intensive, more difficult to converge than eddy viscosity models.

The turbulence model that was chosen for the needs of the intake system case study was the k-omega. The first reason which led me to that decision was that the model

equations do not contain terms which are undefined at the wall, i.e. they can be integrated to the wall without using wall functions in contrast with the k – epsilon model. Additionally, it is accurate and robust for a wide range of boundary layer flows with pressure gradient.

FLUENT offers two varieties of k–ω models:

The Standard k–ω (SKW) model which is most widely adopted in the aerospace and turbo-machinery communities. It contains several sub-models/options of k–ω: compressibility effects, transitional flows andshear-flow corrections.

The Shear Stress Transport k–ω (SSTKW) model (Menter, 1994) which uses a blending function to gradually transit from the standard k–ω model near the wall to a high Reynolds number version of the k–ε model in the outer portion of the boundary layer. It also contains a modified turbulent viscosity formulation to account for the transport effects of the principal turbulent shear stress.

Considering all the above information, the model that was finally chosen so as to model the turbulence is the SST k-omega.

Law of the wall

Turbulent flows are an omnipresent phenomenon in Computational Fluid Dynamics and are significantly affected by the presence of walls, where the viscosity-affected regions have large gradients in the solution variables. An accurate representation of the near wall region determines a successful prediction of wall bounded turbulent flows.

The viscosity of the fluid in motion cannot be neglected in all regions. This leads to a significant condition, the no-slip condition. Flow at the surface of the body is at rest relative to that body. At a certain distance from the body, the viscosity of the flow can again be neglected. This very thin layer close to the body in which the effects of viscosity are important is called the boundary layer. This can also be seen as the layer of fluid in which the tangential component of the velocity of the fluid relative to the body increases from zero at the surface to the free stream value at some distance from the surface.

The behavior of the flow near the wall is a complicated phenomenon and to distinguish the different regions near the wall the concept of wall y+ has been formulated. Thus y+ is a dimensionless quantity, and is distance from the wall measured in terms of viscous lengths.

In a flow bounded by a wall, different scales and physical processes are dominant in the inner portion near the wall, and the outer portion approaching the free stream. These layers are typically known as the inner and outer layers. Considering the flow over a smooth flat plate the boundary layer can be distinguished into two types namely laminar boundary layer and turbulent boundary layer. Since we are dealing with the turbulent boundary layer let us not get into the laminar boundary layer. Typical boundary layer structure over a flat plate is shown below. In between the laminar and turbulent boundary layer there lies a transition region.
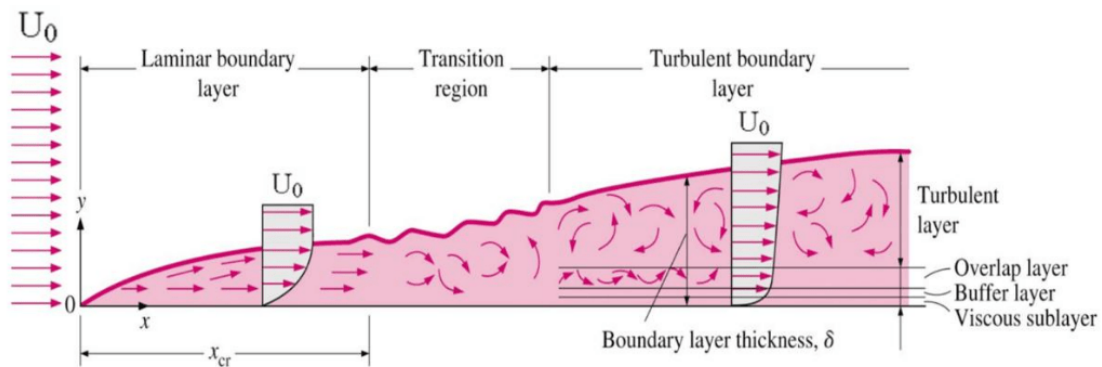

Figure 6 - Boundary layer structure over flat plate

From the above figure it can be seen that in turbulent boundary layer region flow near the wall has been analyzed in terms of three layers:

- The inner layer, or sublayer, where viscous shear dominates
- The outer layer, or defect layer, where large scale turbulent eddy shear dominates
- The overlap layer, or log layer, where velocity profiles exhibit a logarithmic variation.

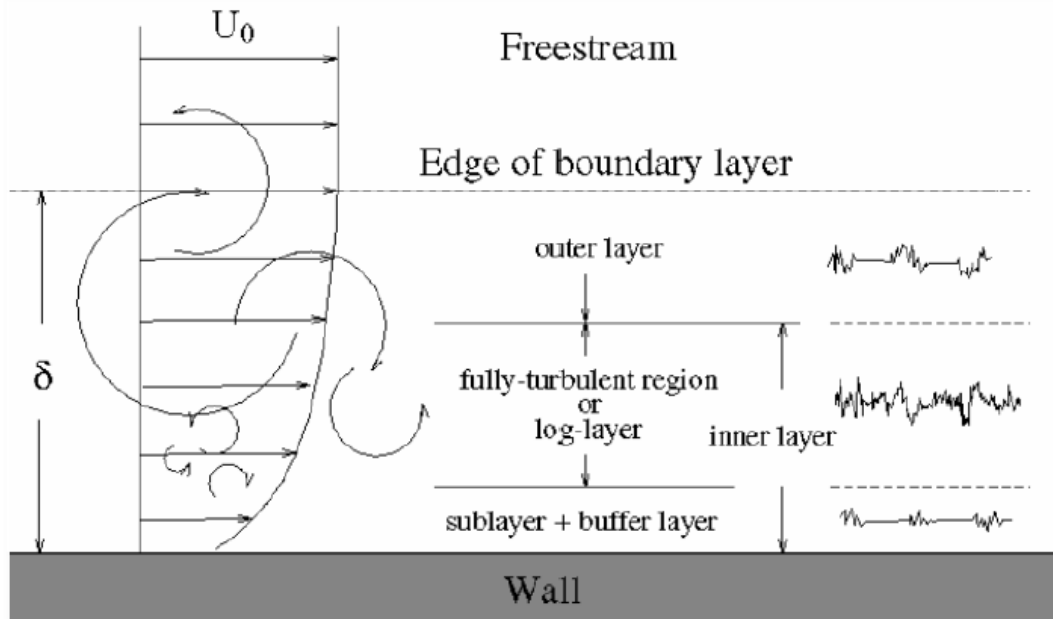 A still clear image of the above is shown below:

Figure 7 - Detailed boundary layer structure

Where Uo is the free stream velocity and δ is the boundary layer thickness, y is the vertical distance measured from the wall.

Turbulent boundary layers are usually described in terms of several non-dimensional parameters. The boundary layer thickness,δ, is the distance from the wall at which viscous effects become negligible and represents the edge of the boundary layer.

Owing to the presence of the solid boundary the flow behavior and turbulent structure are considerably different from free turbulent flows. Dimensional analysis has greatly assisted in correlating the experimental data. In turbulent thin layer flows a Reynolds number based on length scaleL in the flow direction ReL is always very large. This implies that inertia forces are greater than viscous forces at these scales. If we consider Reynolds number on a distance y away from the wall Rey=Uo*y/u , we see that if the value of y is of the order of Rey=Uo*L the above argument holds well. Inertia force dominates far away from the wall. As y also decreases to zero. Just before y reaches zero there will be a range of values of y for which is of the order 1. At this distance from the wall and closer, the viscous forces will be equal in the order of magnitude to the inertia forces or large. To conclude, in flows along solid boundaries there is usually substantial region of inertia dominated flow far away from the wall and a thin layer within which viscous effects are important.

Near to the wall the flow is influenced by the viscous effects and independent of free stream parameters. However the mean flow velocity depends on by y (distance from the wall),ρ (fluid density),μ(viscosity) and wall shear stress.

3. METHODOLOGY

3.1 Workflow

The methodology that was followed in order to reach the final design of the air intake system is presented at the following diagram and explained analytically in the following steps:
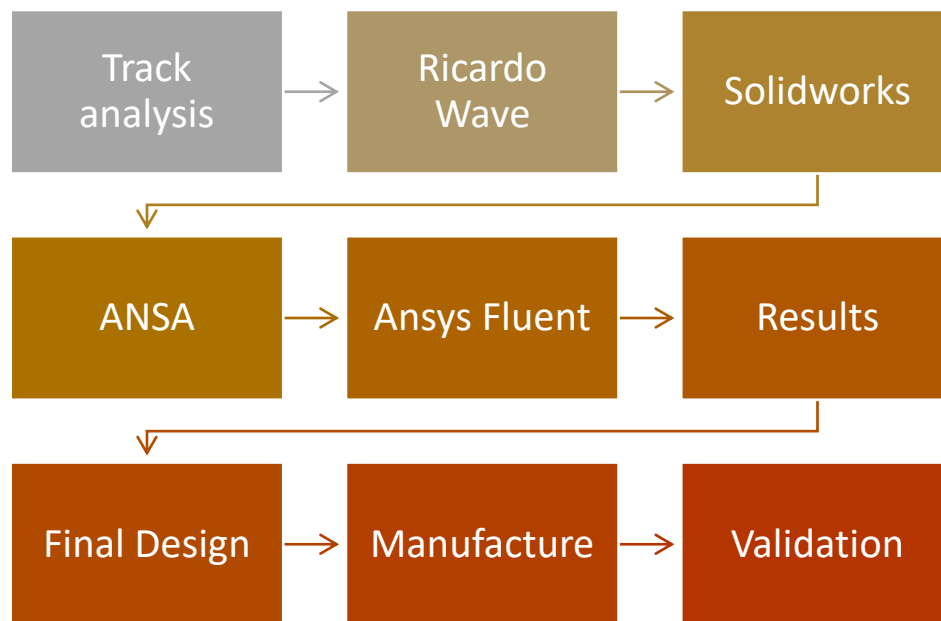

Figure 8 - Thesis methodology

3.2 Software

In order to properly model and simulate the air intake system so as to conclude to the final optimized case, the following software packages were used.

Ricardo Wave

WAVE is a state-of-the-art 1D gas dynamics simulation tool. It is used worldwide in industry sectors including ground transportation, rail, motor sport, marine and power generation. WAVE enables performance and acoustic analyses to be performed for virtually any intake, combustion and exhaust system configuration. WAVE simulation software solves the 1D form of the Navier-Stokes equations governing the transfer of mass, momentum and energy for compressible gas flows, and includes sub-models for combustion and emissions.

Solidworks

SolidWorks is a solid modeling computer-aided design (CAD) and computer-aided engineering (CAE) computer program featuring integrated analytical tools and design automation to help stimulate physical behaviour such as kinematics, dynamics, stress, deflection, vibration, temperatures or fluid flow to suit all types of design.

ANSA

ANSA is an advanced multidisciplinary CAE pre-processing tool that provides all the necessary functionality for full-model build up, from CAD data to ready-to-run solver input file, in a single integrated environment. ANSA is the users' preference due to its wide range of features and tools that meet their needs.

Ansys

Fluent software contains the broad, physical modeling capabilities needed to model flow, turbulence, heat transfer and reactions for industrial applications. These range from air flow over an aircraft wing to combustion in a furnace, from bubble columns to oil platforms, from blood flow to semiconductor manufacturing and from clean room design to wastewater treatment plants. Fluent spans an expansive range, including special models, with capabilities to model in-cylinder combustion, aero-acoustics, turbomachinery and multiphase systems.

META

META provides a broad range of functionality that can successfully address even the most demanding post processing requirements for structural and CFD analyses. It supports results from all popular solvers used in structural analysis as well as CFD results from Fluent and OpenFOAM.

3.3 Engine Specifications

As stated before, the engine applied on the racecar is Honda CBR 600rr and features the following:

Manufacturer/Model	2007 Honda CBR 600rr
Number of cylinders	4
Displacement (cc)	602,9
Compression	13:01
Bore (mm)	67,2
Stroke (mm)	42,5
Peak power @ 10600 rpm (kW)	63
Peak torque @ 8900 rpm (Nm)	61
Induction	Natural

Figure 9 - Engine Specifications

3.4 Track Analysis

Firstly, the prototype was tested in a circuit similar to the one faced at the competition site. The goal was to obtain data regarding the engine speed range most used along the run.

Since the main characteristic of this circuit is the intensive presence of chicanes and slaloms, the engine is used in a very wide range of speeds, from low to high ones. It is possible to state that the most recurrent speeds lie within the region between 5000 and 11000 rpm.

In parallel, analyzing the dynamometer tests that were performed in last year's car (figure 10) showed that in 6000rpm and 7500rpm the torque curve needed to be smoothed. Additionally, the curve as a whole was noticeably low, considering the performance needs of the car, so the team concluded to the change of the intake camshafts' profile. As a consequence a new intake system had to be designed according to the camshafts' characteristics. Moreover, it was observed that the engine should be provided with more available air at 6800rpm which was normally the turn exit speed, so this was decided to be the resonance tuning value.
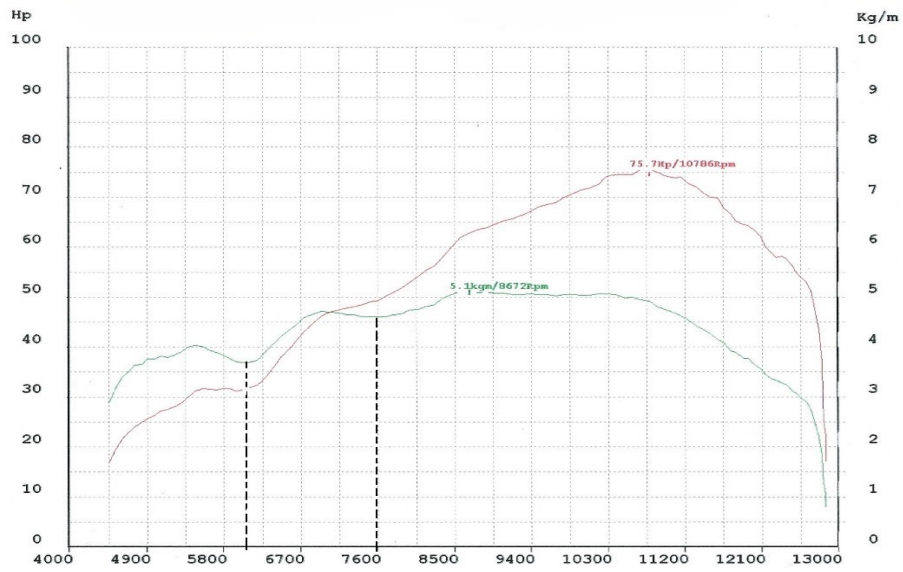
Figure 10 - Dynamometer torque and horsepower diagrams

3.5 Design

Restrictor

According to the theory behind the restrictor's physics and after changing some of the geometric variables of restrictor at Ricardo Wave, the dimensions of the Converging Diverging nozzle on which the process should be focused, are: the diameter of the inlet, the converging angle, the diameter of the outlet and the diverging angle.
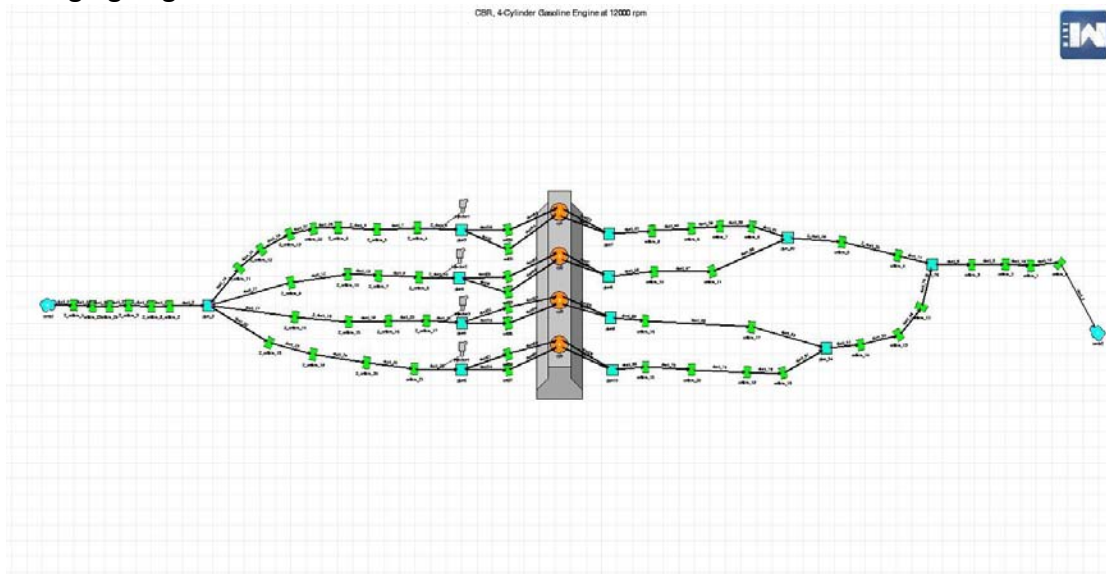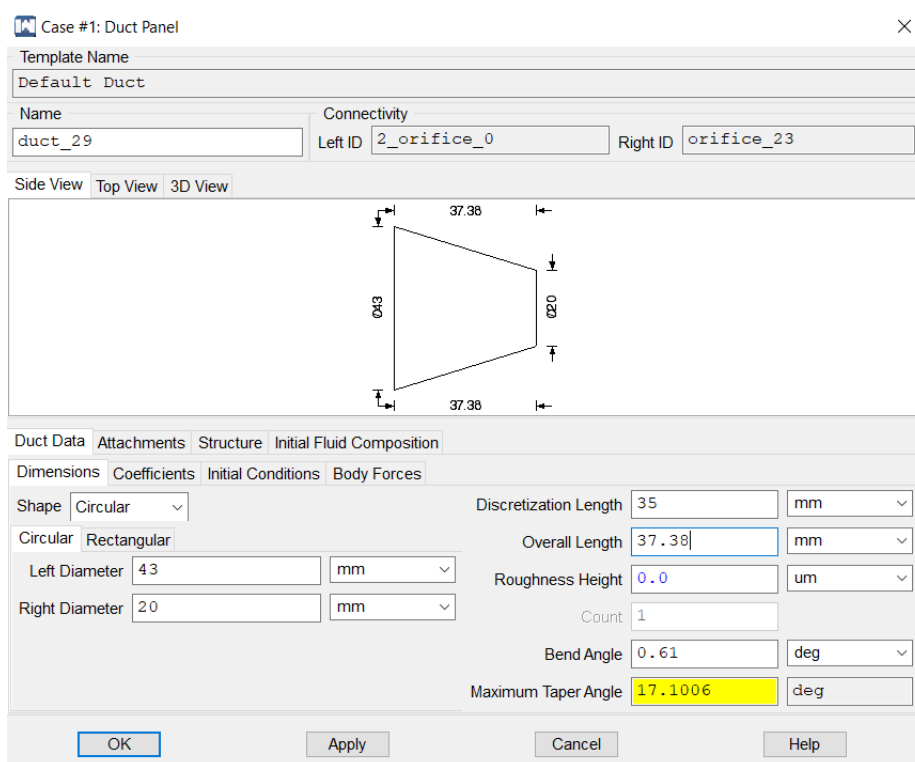

Figure 11- Ricardo Wave Model

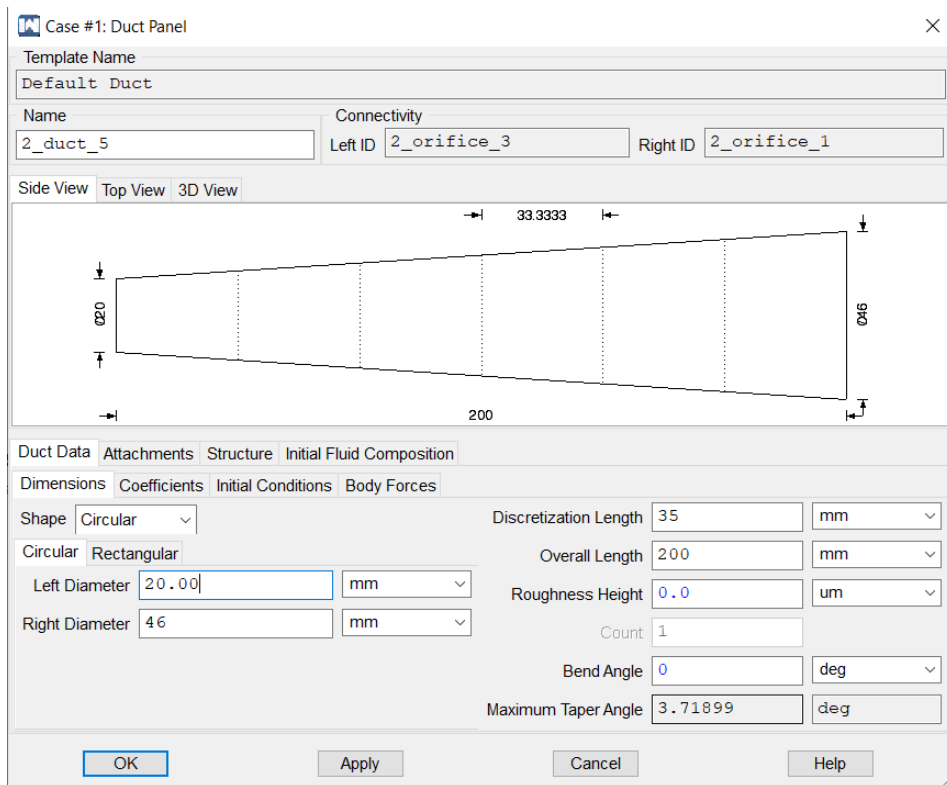**Figure 12 - Restrictor modeling at Ricardo Wave**

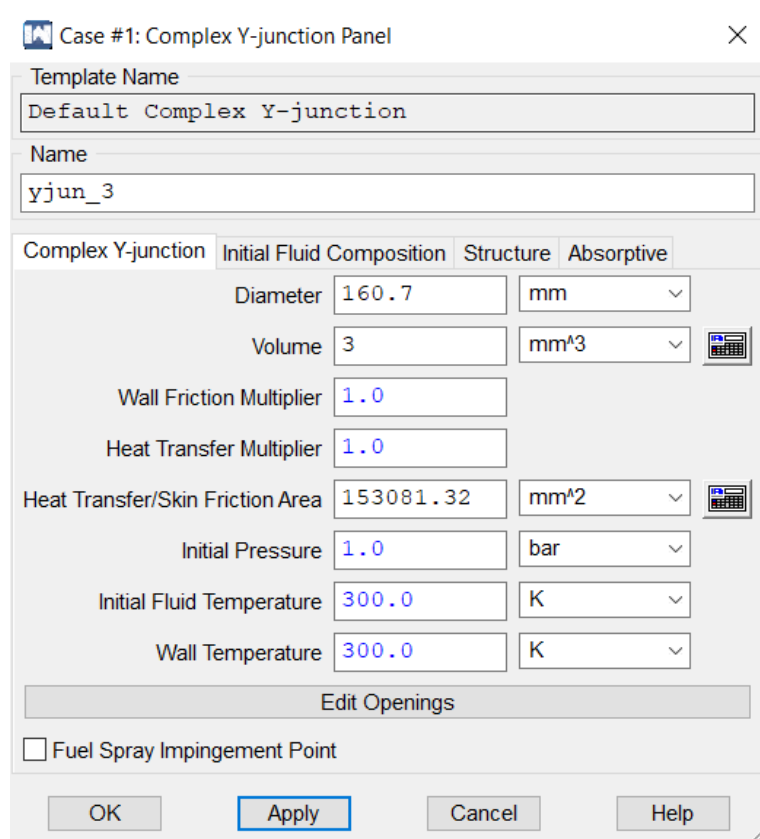**Figure 13 - Restrictor Modeling at Ricardo Wave (part 2)**

Figure 14 - Plenum modeling at Ricardo Wave

For each one of these variables, an upper and a lower value was set and then with a FORTRAN calculation, all the possible combinations of values were found:

```fortran
restrictor.f90    ×
(Global Scope)
program restrictor

    implicit none
    real:: InR, OutR, InAng, OutAng
    integer:: i

    InAng=17.0
    i=0

    Do OutR=22,30,1
        Do OutAng=3.5,6,0.5
            Do InR=19,21,1
                i=i+1
                write(*,*) InR, InAng, OutR, OutAng
            end do
        end do
    end do

    write(*,*) i

end program
```

Figure 15 - Restrictor's possible angles and diameters calculation

After that, a parametric design at Solidworks was built, so as to have easy access at all the different restrictor's geometries.
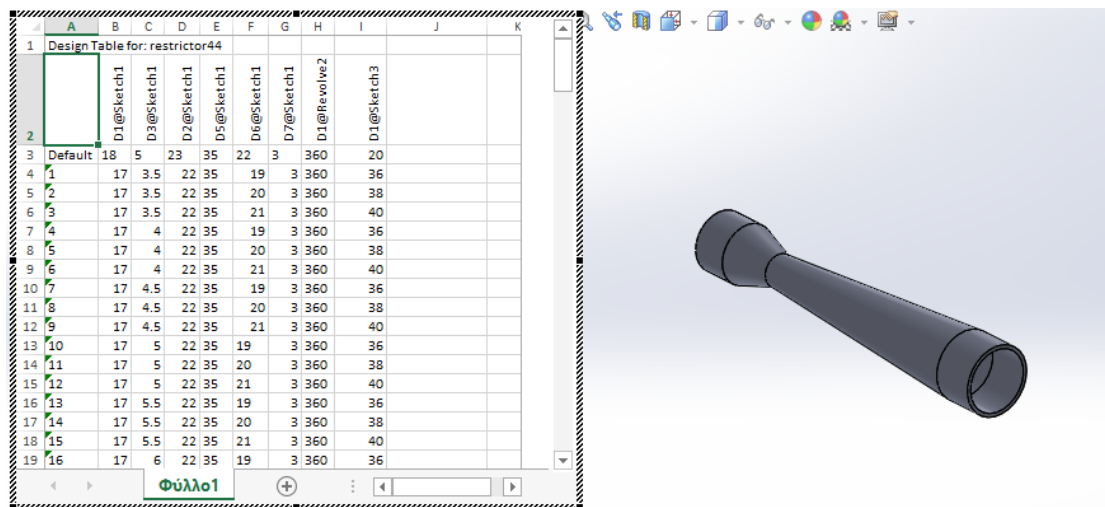

Figure 16 - Restictor designs

Finally, various concepts featuring different curves on the plenum and the ports were designed so as the air flow inside them to be tested with the Computational Fluid Dynamics procedure.

Plenum & Runners

Further up with the plenum and the runners, the main goal was to achieve resonance tuning at 6800 rpm, so as to have available air at the turn exit, a problem that the last year's racecar faced with the applicable engine. Additionally, equal flow distribution in the four cylinders was the following target, as well as minimal air losses through a well – integrated symmetrical intake system design.

Plenum

At first, the capacity of the plenum had to be decided. A relatively large plenum favors the horsepower, because of the provided air availability at any time. On the other side, a very large plenum can cause problems in throttle response due to the inertia of the static air, when the throttle pedal is pushed, fact that can be tested only on the track. Due to the difficulty to construct and test a number of different plenums on track or at the dynamometer, some experiments were conducted with the aid of Ricardo Wave by changing the capacity of plenum and observing the results. Finally, we concluded that the golden section of the volume and the throttle response was 3 liters.
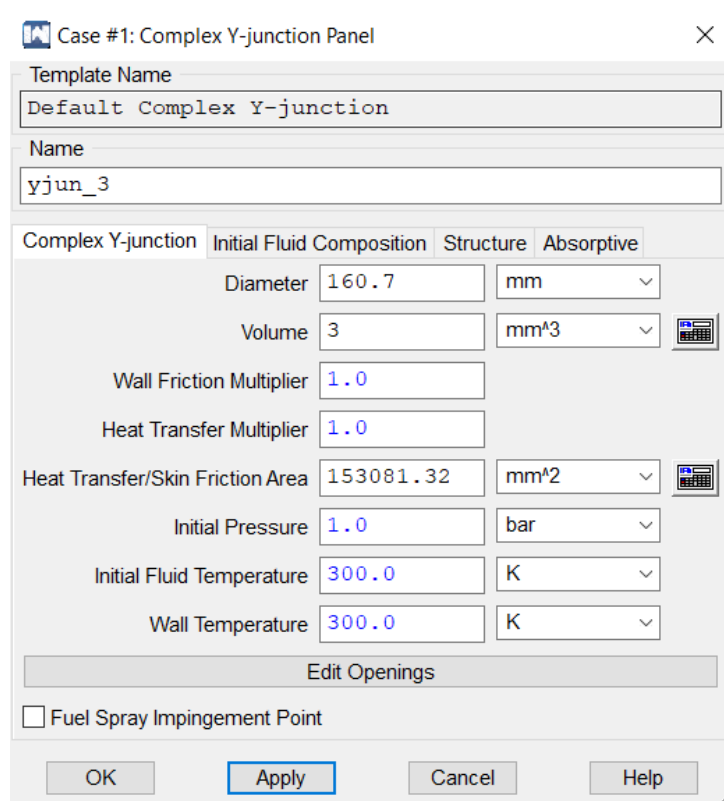

Figure 17- Plenum specifications at Ricardo Wave

As for the shape, a fully symmetrical geometry with smooth curves was chosen so as to achieve good flow distribution in the four cylinders and minimize losses. A significant factor that affected the chosen curves that were used to shape the

35

plenum was the manufacturing process that had to be used. According with the team's limited resources the intake system had to be constructed using aluminum fact that restricted significantly the design characteristics. Finally, a steady state fluid model was set in order to test the flow uniformity inside the whole intake system. Although the flow inside is inherently unsteady, we preferred the steady state model to decide the general intake system geometrical characteristics, so as to reduce computational time requirements.

Runners

When an engine is running, there are high and low pressure waves moving in the manifold caused by the inertia of the air and the opening and closing of the valves. As already explained, the idea of runner tuning is to have a high-pressure wave approach the intake valve before it closes or just as it opens, forcing in a little more intake charge. In order to improve our engine's performance at 6800 rpm, so as to increase the availability of air at the turn exit, we concluded to the following length:

L = ((ECD × 0.25 × V × 2) ÷ (rpm × RV)) - ½D, where:
ECD = Effective Cam Duration
RV = Reflective Value = 4
D = Runner Diameter = 35   **Equation 14**

The selection of the diameter, was a result of testing different combinations at the Ricardo Wave. We opted for a runner geometry with slightly different diameter at the top and at the bottom, for the sake of further helping the repletion of the cylinder, by achieving a high velocity at the back of the valve.

3.6 Mesh generation

In order to proceed with the Computational Fluid Dynamics calculations, a detailed mesh generation was needed so as to capture the various phenomena inside the system. The mesh was generated using the ANSA pre-processor.

At first, the created restrictor designs were entered in order for their geometry to get cleaned up and be prepared for the meshing process:
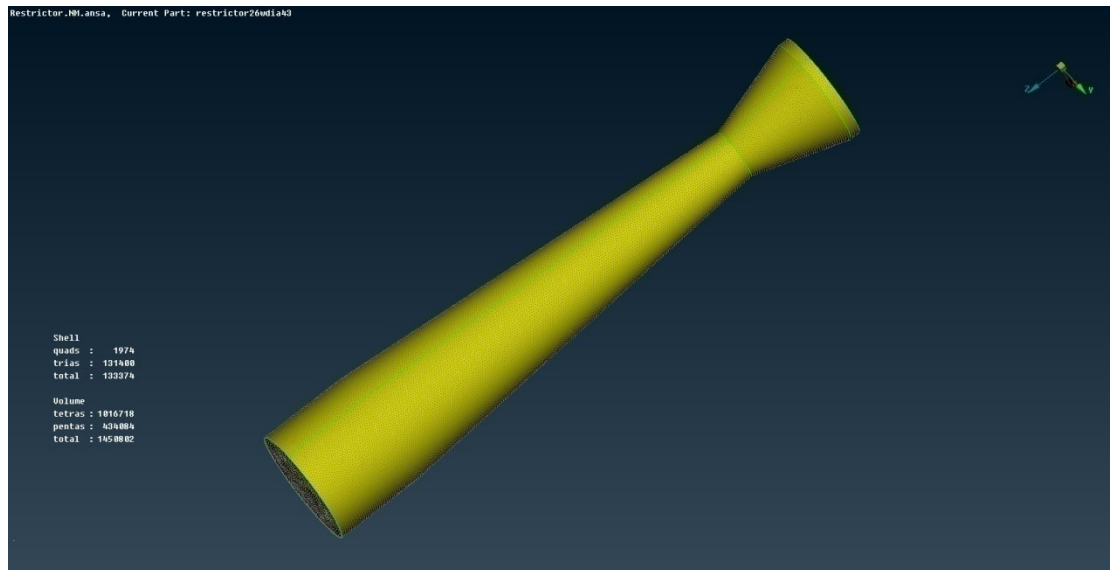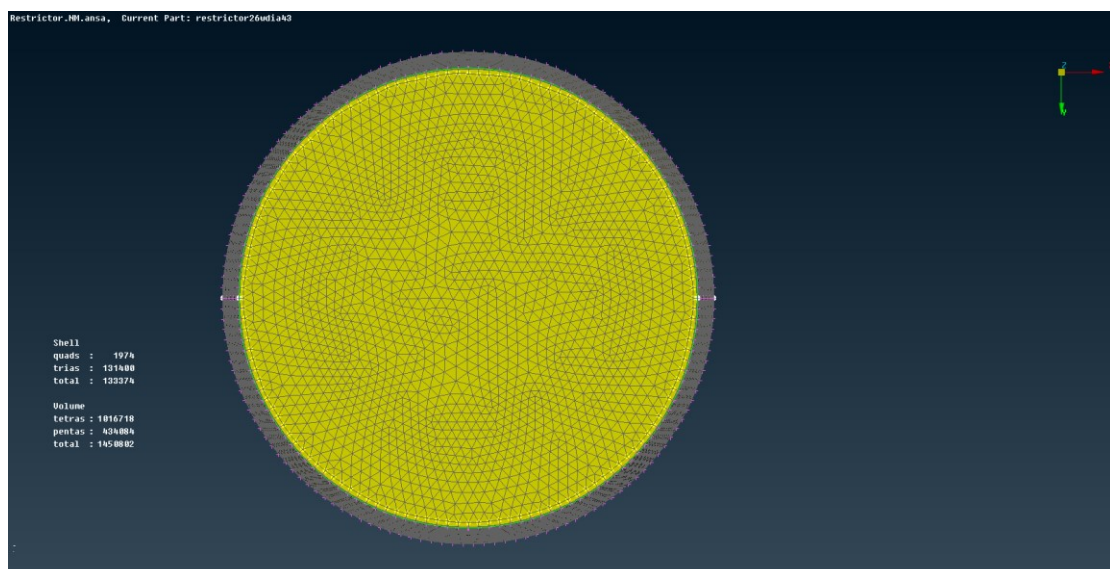

Figure 18 - Restrictor geometry cleaned up

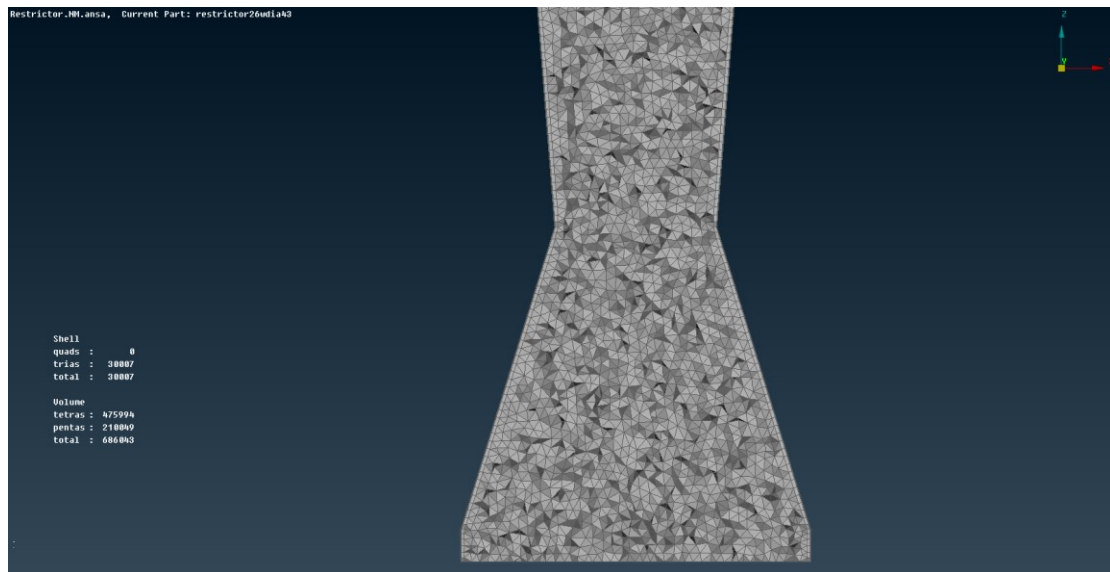**Figure 19 - Restrictor mesh generation (top view)**

Figure 20 - Restrictor mesh generation (cross section)

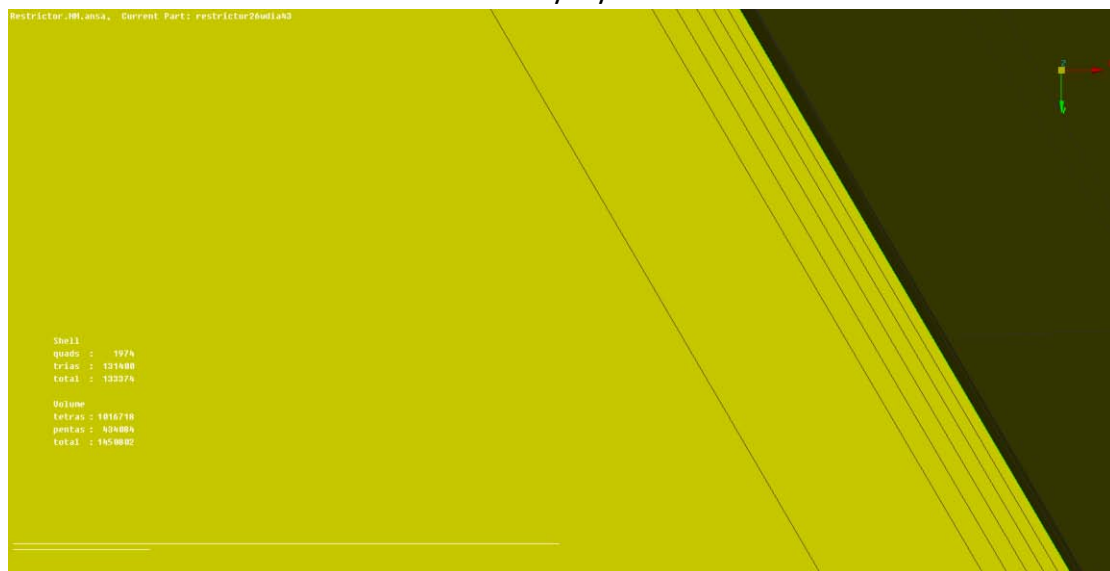A fine mesh was created and the boundary layer was discretized as follows:

Figure 21 - Boundary layer discretization
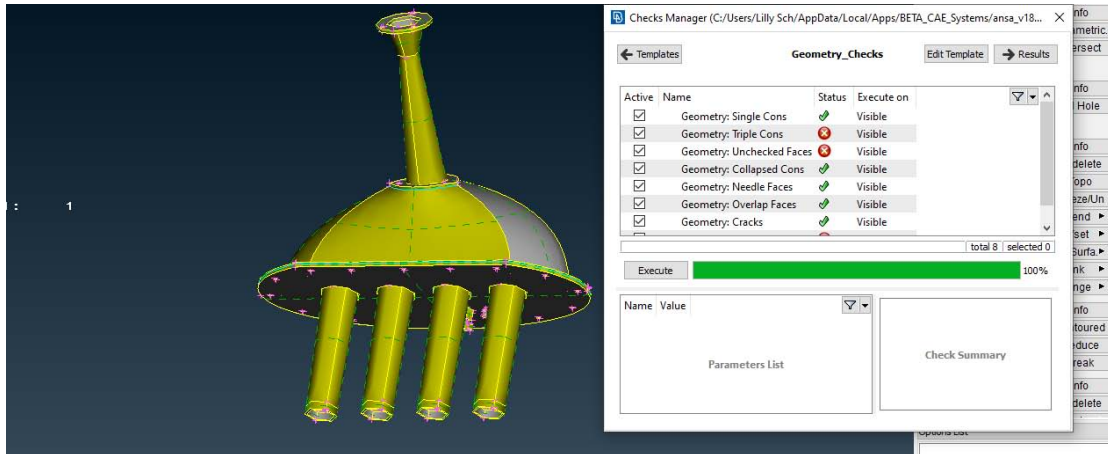
Afterwards, the design of the whole air intake was entered:

38

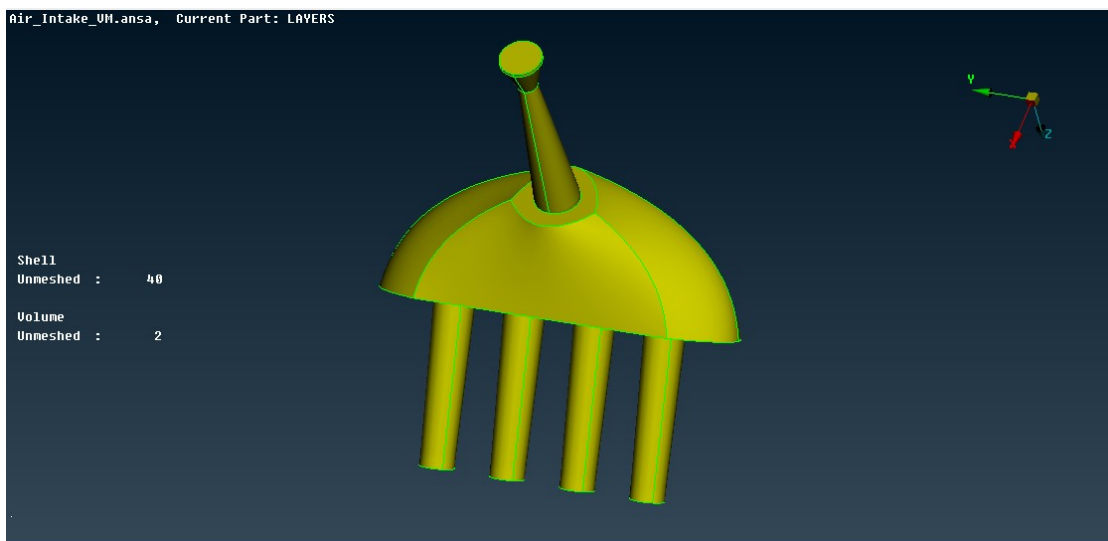**Figure 22 - Intake system before cleanup**

Figure 23 - Intake system cleaned up

After the geometry was cleaned the part was divided in three PIDs

- Restrictor
- Plenum and bellmouths
- Runners

and the surface mesh, the layers over the wall and finally the volume mesh were generated:
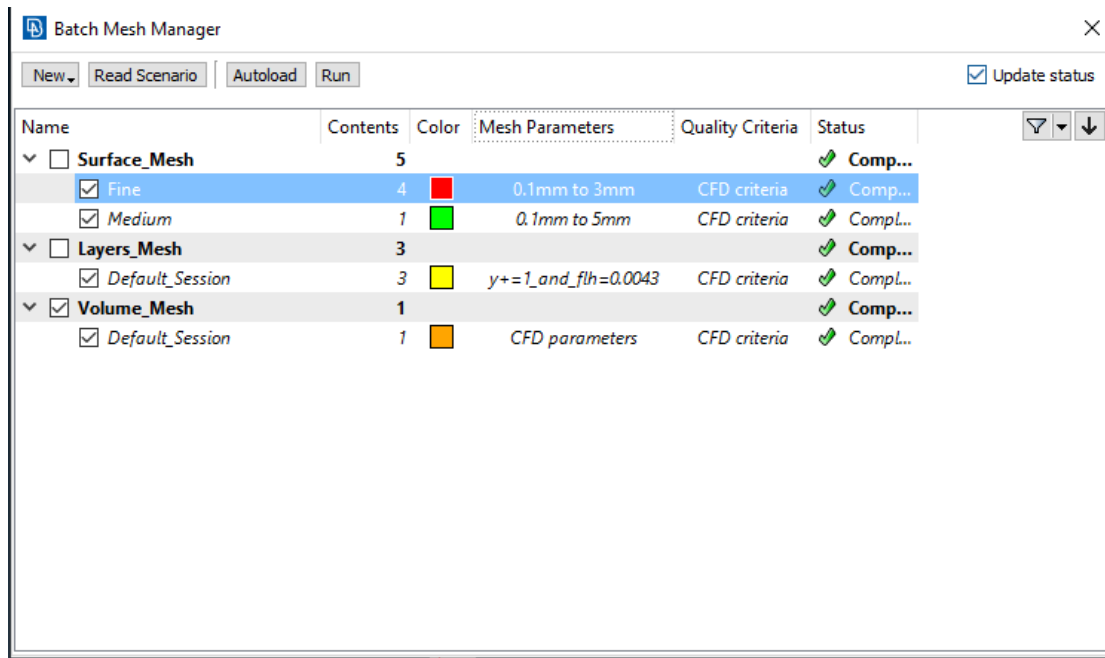
Figure 24 - Batch mesh

The first meshing approach was a medium grid:
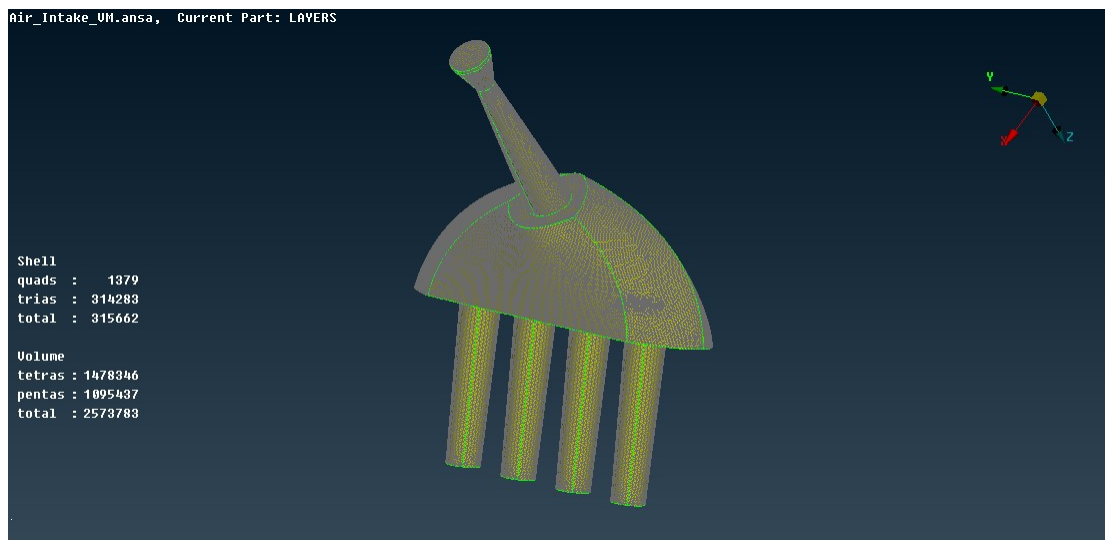
Figure 25 - Medium meshing

By observing the details of the mesh it was concluded that the mesh generation around the bellmouth geometry caused some issues at the plenum's geometry:
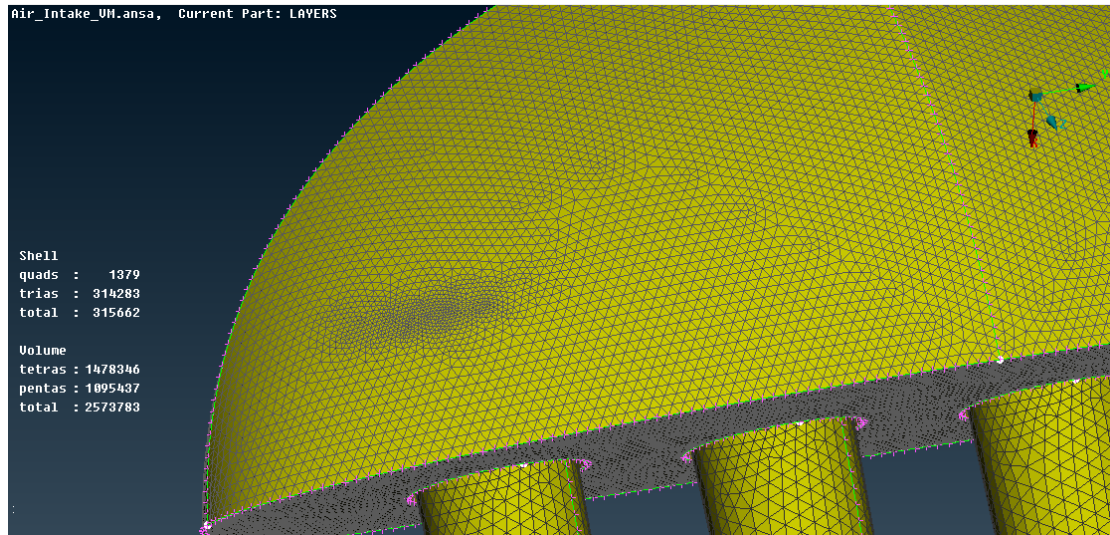
Figure 26 - Problematic meshing
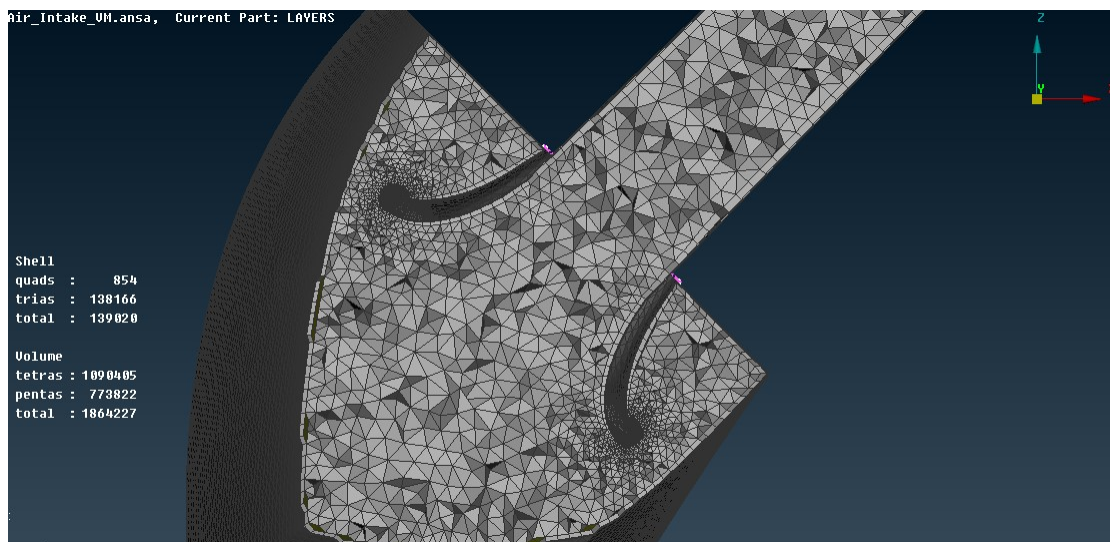
Figure 27 - Problematic meshing (cross section)

In order to solve the issue, another PID was created so as to differentiate the plenum and the bellmouths' geometry. The mesh was generated again and as can be seen it became smooth:

Shell
quads :   1386
trias : 330906
total : 332292

Volume
tetras : 1659099
pentas : 1153208
total : 2812307

Figure 28 - Problematic meshing solution

Afterwards, a finer mesh was created so as to simulate the air intake system in more
detail:

Shell
quads :   2702
trias : 647690
total : 650392

Volume
tetras : 2698131
pentas : 2249142
total : 4947273
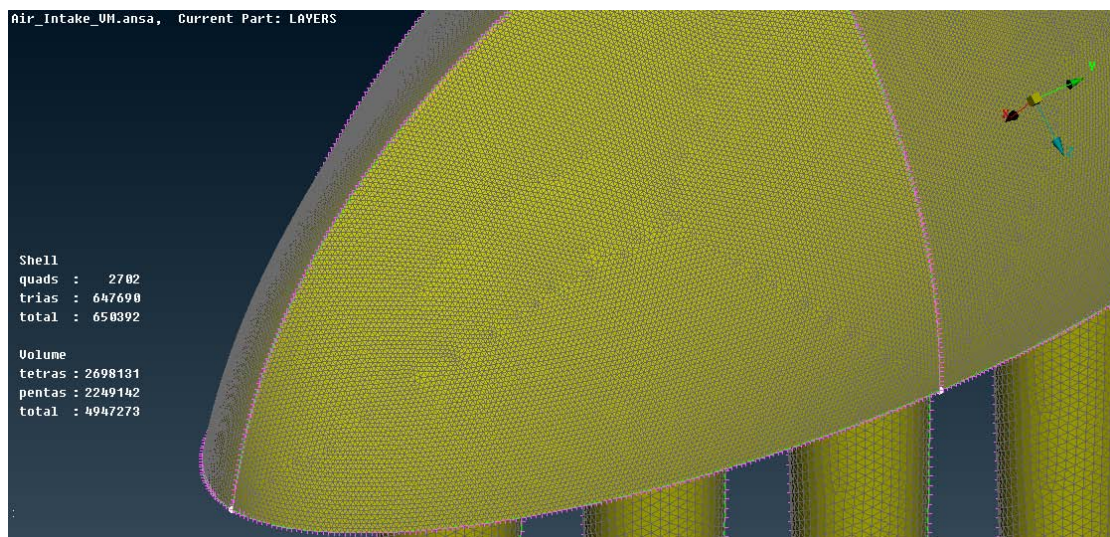
Figure 29 - Fine meshing generation

3.7 Simulation

Because of all the reasons explained in the literature review, the following setup was used in order to receive results and finally optimize the airflow inside the intake system:

Model

1) Pressure based solver
2) Energy equation
3) K-omega SST equations
4) Material: Ideal gas
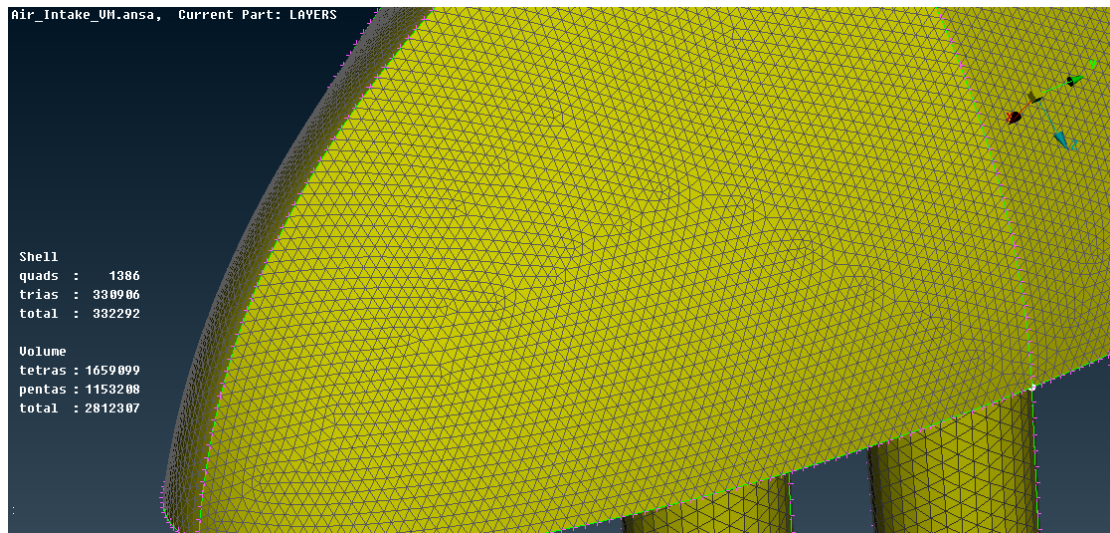5) Operating conditions
   - 0 atm
   - 300 K
6) Solution methods
   - Coupled scheme
   - Gradient → Least squares cell based
   - Pressure → Second Order
   - Density Momentum → Second Order Upwind
   - Turbulent Kinetic Energy → Second Order Upwind
   - Specific Dissipation Rate → Second Order Upwind
   - Energy → Second Order Upwind
   - Pseudotransient
7) Solution Initialization → Hybrid Initialization

Boundary Conditions

   - Pressure Inlet: 101325 Pa
   - Pressure Outlet: 90000 Pa

4. RESULTS

Restrictor

In order to classify the CFD results in an efficient way that would lead to the most convenient restrictor choice, the following Excel tables were filled with the mass flow rate, the pressure drop and the length of each restrictor geometry:

Inlet radius = 19mm :

mfr	3.5	4	4.5	5	5.5	6
22	0.074311	0.073753	-	-	0.068546	0.068519
23	0.074533	0.073927	0.073225	-	0.067793	0.067774
24	0.073703	0.072862	0.073291	-	-	0.066757
25	0.073913	0.073154	0.070860	0.071323	0.066837	0.065807
26	0.074122	0.073398	0.072163	0.070601	0.069925	0.064706
27	0.074308	0.072391	0.072391	0.066791	0.064628	0.064948
28	0.073483	0.072550	0.071426	-	0.067704	0.064867
29	0.074544	0.073846	0.071573	0.070386	0.067846	0.066508
30	0.074617	0.073976	0.719660	-	-	-

pressure drop	3.5	4	4.5	5	5.5	6
22	13000	11000	-	-	-	-
23	12900	10300	9800	-	-	-
24	12900	10600	-	-	-	-
25	12500	11800	-	-	-	-
26	12200	11200	9300	-	-	-
27	12100	-	10100	-	-	-
28	12200	10900	-	-	-	-
29	9300	12000	-	-	-	-
30	-	12000	-	-	-	-

best	pd	mfr	length
79	9300	0.072163	297.76
25	9800	0.073225	259.62
97	10100	0.072391	310.44
22	10300	0.073927	280.35
40	10600	0.072862	294.65
112	10900	0.072550	351.9
127	9300	0.074544	405.08

length	3.5	4	4.5	5	5.5	6
22	290.64	266.05	-	-	-	-
23	306.99	280.35	259.62	-	-	-
24	323.34	294.65	-	-	-	-
25	339.69	308.95	-	-	-	-
26	356.10	323.25	297.76	-	-	-
27	372.39		310.44	-	-	-
28	388.74	351.90	-	-	-	-
29	405.08	366.15	-	-	-	-
30	421.43	380.45	-	-	-	-

Inlet radius = 20mm :

mfr	3.5	4	4.5	5	5.5	6
22	0.073632	0.073098	-	0.07119	0.068734	0.068019
23	0.073955	0.07339	0.072321	-	0.066746	0.066613
24	0.074209	0.073492	0.071149	-	-	0.065723
25	0.073346	0.072432	0.071367	0.069602	0.070413	0.066384
26	0.073532	0.072639	0.071525	0.070507	0.065933	0.067913
27	0.073728	0.072853	0.071712	-	-	-
28	0.074864	0.072985	0.071902	-	-	-
29	0.073977	0.073125	0.07029	-	-	-
30	0.074112	0.073288	0.072215	0.068928	0.066316	-

pressure drop	3.5	4	4.5	5	5.5	6
22	12000	11000	-	-	-	-
23	12300	11000	8900	-	-	-
24	12900	11400	-	-	-	-
25	12600	10800	-	-	-	-
26	12300	10300	-	-	-	-
27	11600	11100	-	-	-	-
28	12800	11100	-	-	-	-
29	-	11000	-	-	-	-
30	-	11800	8500	-	-	-

best	pd	mfr	length
152	8500	0.072215	351.9
26	8900	0.072321	262.89
77	10300	0.072639	326.53
59	10800	0.072432	312.22

length	3.5	4	4.5	5	5.5	6
22	293.91	269.32	-	-	-	-
23	310.26	283.62	262.89	-	-	-
24	326.61	297.92	-	-	-	-
25	342.96	312.22	-	-	-	-
26	-	326.53	-	-	-	-
27	375.66	-	-	-	-	-
28	392.01	-	-	-	-	-
29	408.45	369.42	-	-	-	-
30	424.72	383.72	351.9	-	-	-

Inlet radius = 21mm :

mfr	3.5	4	4.5	5	5.5	6
22	0.074374	-	-	0.068813	0.067572	0.06304
23	-	0.072355	0.071338	0.071776	0.065544	0.066323
24	0.073434	0.072561	0.071528	0.070555	0.067531	0.06678
25	0.073661	0.072822	0.071892	0.069393	0.067402	0.066916
26	0.073869	0.073027	0.071945	0.068883	0.067458	-
27	0.074009	0.07316	0.071189	-	-	-
28	0.074158	0.073347	0.071352	0.068209	-	-
29	0.074303	0.073539	-	-	-	-
30	0.073705	0.072833	0.072581	-	-	0.064623

pressure drop	3.5	4	4.5	5	5.5	6
22	11200	-	-	-	-	-
23	-	-	-	-	-	-
24	12700	-	8900	-	-	-
25	12200	10900	-	-	-	-
26	13100	11200	-	-	-	-
27	12500	10700	-	-	-	-
28	13000	11000	-	-	-	-
29	-	11000	-	-	-	-
30	-	-	-	-	-	-

best	pd	mfr	length
45	8900	0.071528	278.89
96	10700	0.07316	344.09
60	10900	0.072822	315.49

length	3.5	4	4.5	5	5.5	6
22	297.18	-	-	-	-	-
23	-	-	-	-	-	-
24	329.88	-	278.89	-	-	-
25	346.23	315.49	-	-	-	-
26	362.58	329.79	-	-	-	-
27	378.93	344.09	-	-	-	-
28	395.28	358.39	-	-	-	-
29	411.63	372.69	-	-	-	-
30	427.98	-	-	-	-	-

Finally, combining all the above data along with the velocity magnitude streamlines of the CFD post – process the most suitable results were found to be the following:
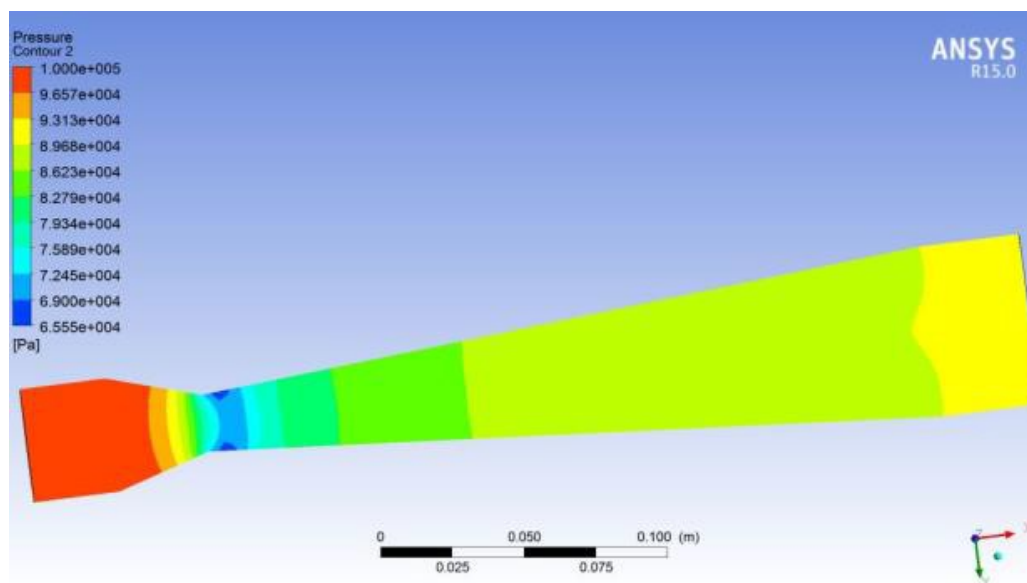

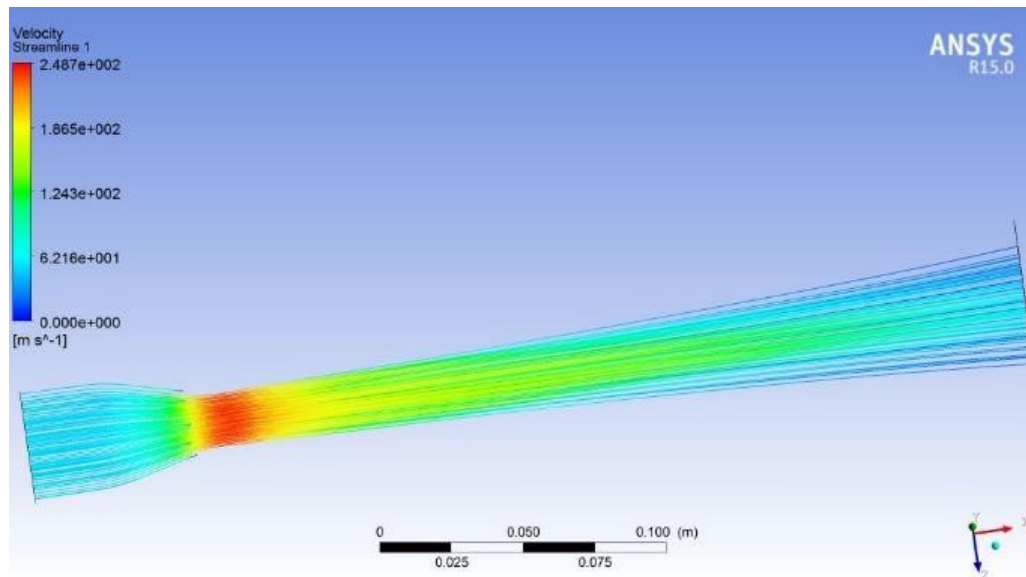**Figure 30 - Restrictor post processing - Pressure distribution**

45

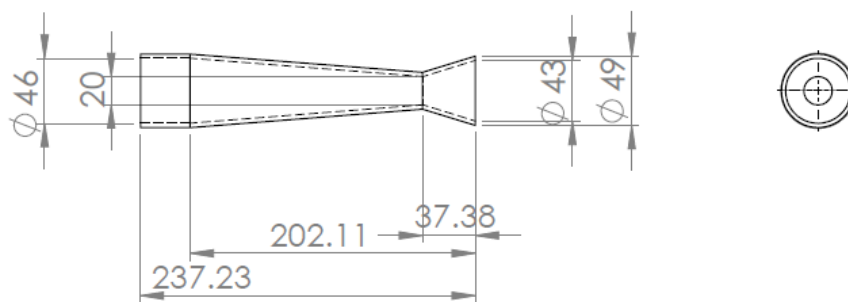**Figure 31- Restrictor post processing - Velocity streamlines**

Figure 32 - Restrictor final design drawing

Concerning the whole intake system, after creating a number of different design concepts the following two were the final ones, before the concluding decision. They both feature the same plenum and runners with their main difference to be found at the restrictor. At the first concept, the restrictor is cut at the contact patch with the plenum, while at the second a tubular piece follows the restrictor, entering the plenum.
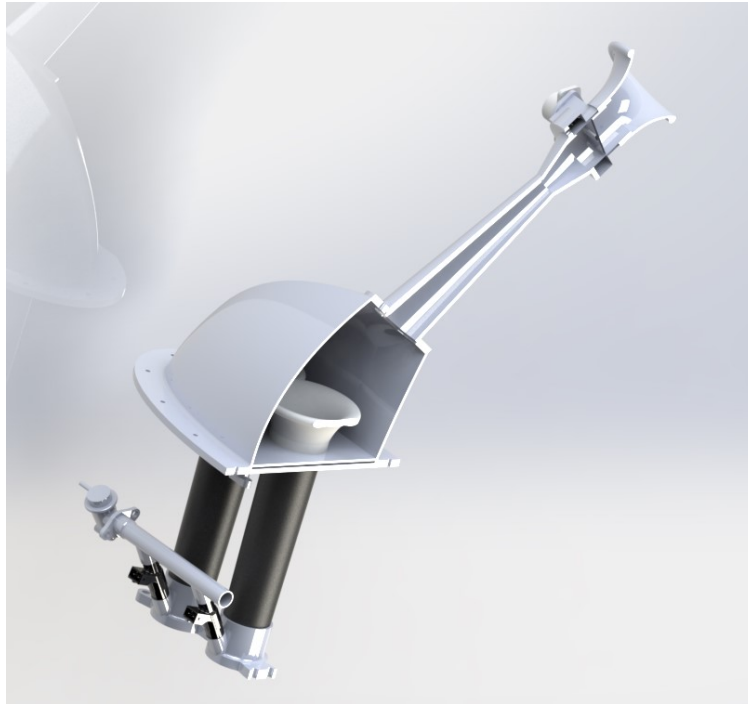
Figure 33 - First intake system design

Figure 34 - First intake system design

Figure 35 - Second intake system design

Figure 36 - Second intake system design

So, the final results are the following. Due to the fact that all the cases were run at steady state conditions, the results are not as representative as if they were if a transient model had been developed. However, the steady state approach is capable of providing us with qualitative comparisons.

Each intake and exhaust valve is open for a subtle amount of time so the first simulation was run with all the four runners open.
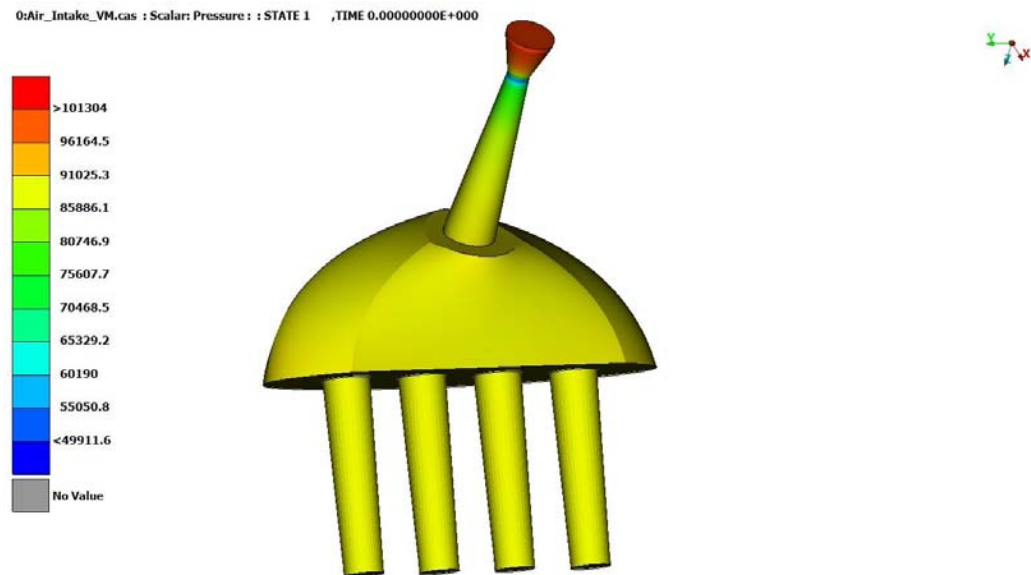
Figure 37 - CFD Case 1
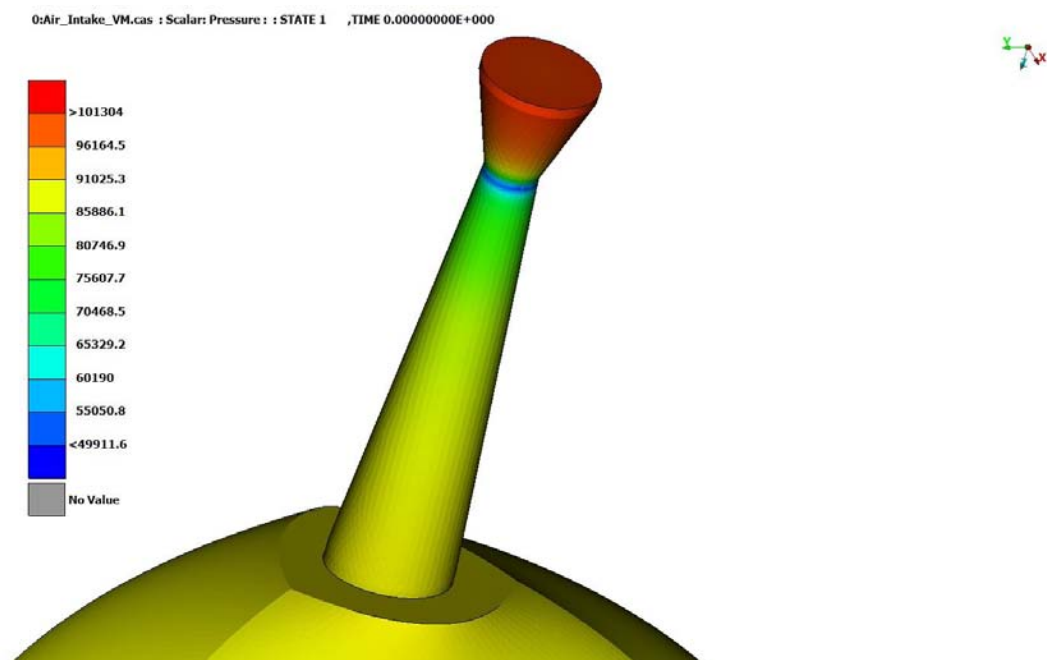
Figure 38 - CFD Case 1

0:Air_Intake_VM.cas : Scalar: Pressure : : STATE 1   ,TIME 0.00000000E+000
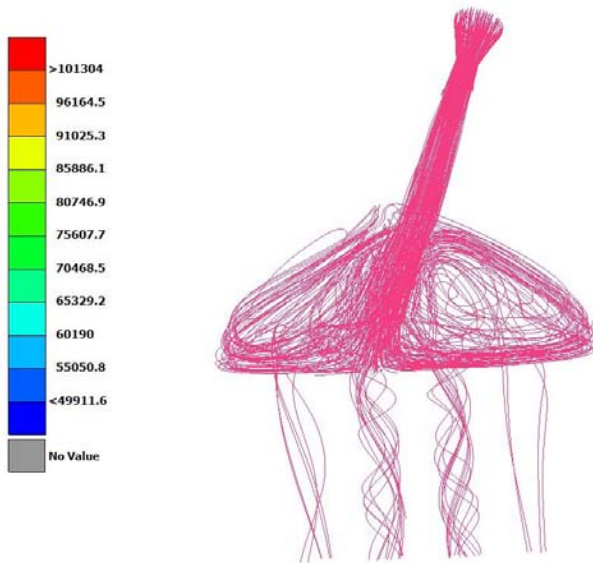
Figure 39 - CFD Case 1

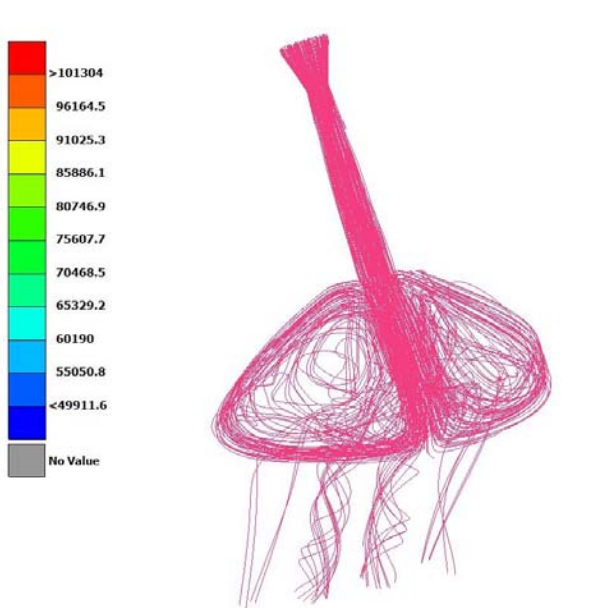0:Air_Intake_VM.cas : Scalar: Pressure : : STATE 1   ,TIME 0.00000000E+000

Figure 40 - CFD Case 1

As stated before, one of the intake system's goals is to provide all the four cylinders with equal amount of air , fact that is practically impossible. From the streamlines though a symmetrical distribution of air portions can be noticed inside the intake system.

More specifically, keeping the first runner open and the other ones closed brings the following pressure distribution and velocity results. The meshing that was used was the medium one.
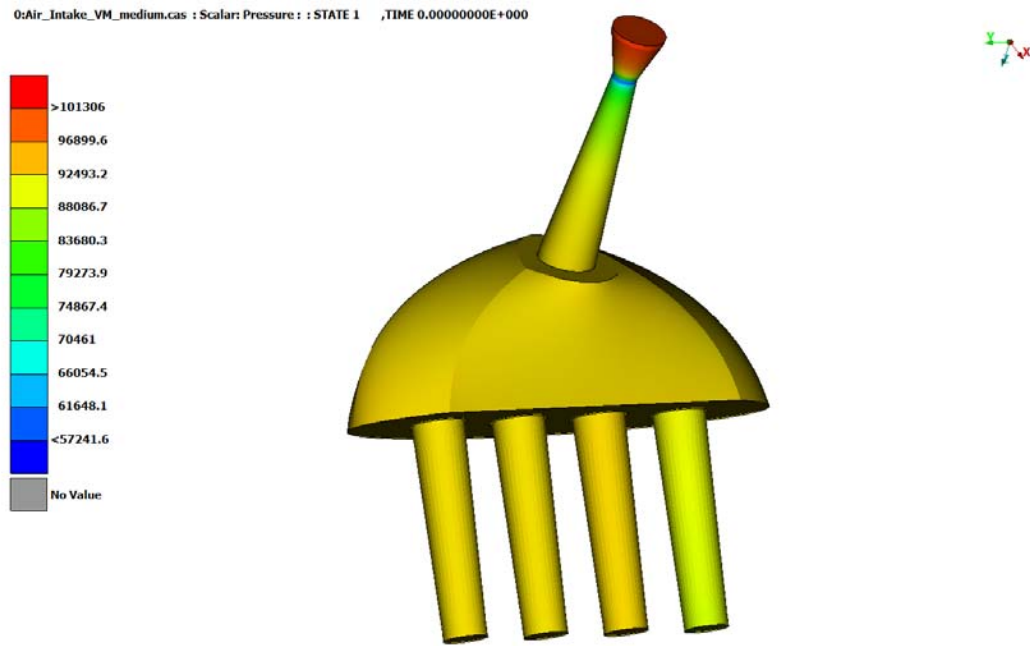
50

Figure 41 - CFD Case 2

Figure 42 - CFD Case 2

Continuing with the medium mesh approach, this time the focus was given at the second runner so as to receive data for the differences between the middle runners with the outer ones.

51

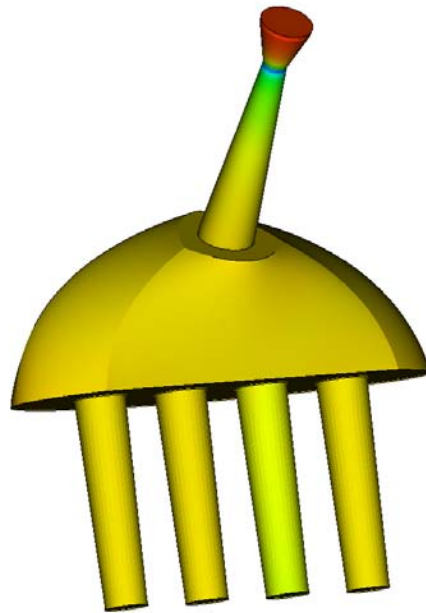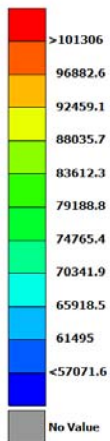0:Air_Intake_VM_medium.cas : Scalar: Pressure : : STATE 1   ,TIME 0.00000000E+000

Figure 43 - CFD Case 2

0:Air_Intake_VM_medium.cas : STATE 1   ,TIME 0.00000000E+000

Figure 44 - CFD Case 2

Then the same procedure was followed with the finer and more detailed mesh in order to observe the differences in the results and decide if there is an actual need for the fine mesh use or the medium mesh is capable of giving accurate enough data.

52

0:Air_Intake_VM-1-03000.cas : Scalar: Pressure : : STATE 1   ,TIME 0.00000000E+000

>101299
96588.9
91878.4
87167.9
82457.4
77746.9
73036.4
68325.9
63615.4
58904.9
<54194.4

No Value

Figure 45 - CFD Case 3

Afterwards the same setup was implemented on the second approach with the restrictor part entering the plenum so as to compare the results with the previous concept's ones. At first, a medium mesh was used.

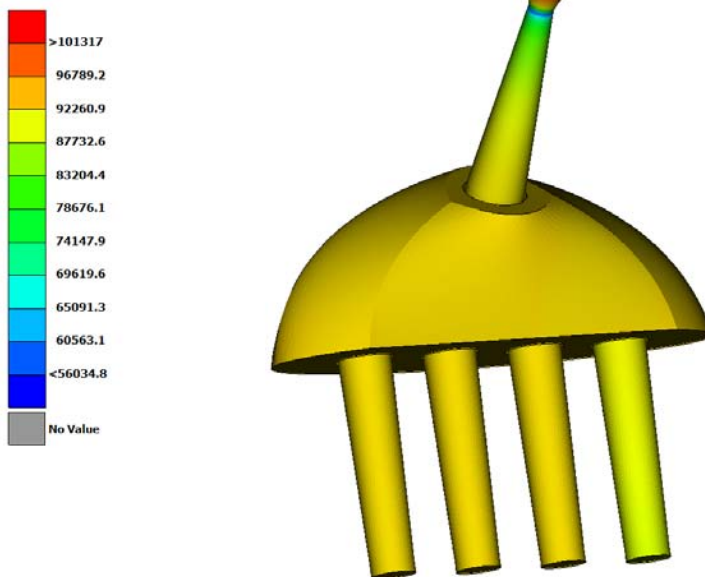0:Full_Res_Medium_Out1.cas : Scalar: Pressure : : STATE 1   ,TIME 0.00000000E+000

>101317
96789.2
92260.9
87732.6
83204.4
78676.1
74147.9
69619.6
65091.3
60563.1
<56034.8

No Value

Figure 46 - CFD Case 5

0:Full_Res_Medium_Out1.cas : STATE 1   ,TIME 0.00000000E+000

Figure 47 - CFD Case 5

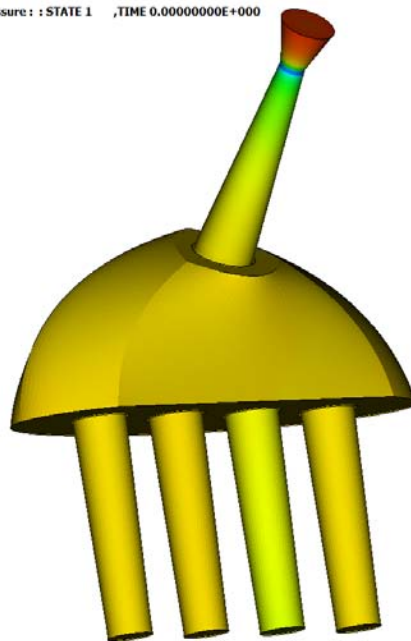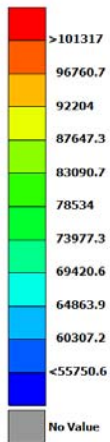0:Full_Res_Medium_Out2.cas : Scalar: Pressure : : STATE 1   ,TIME 0.00000000E+000

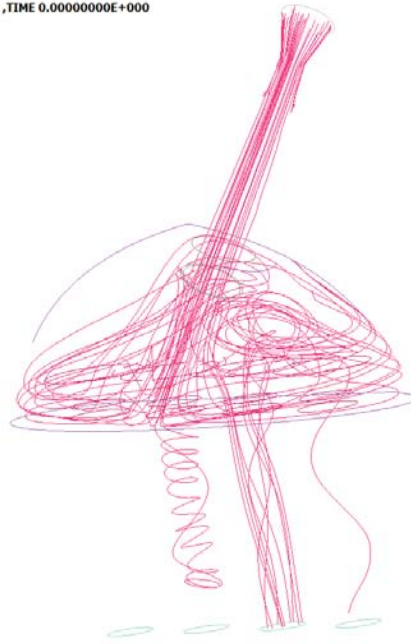| >101317 |
| 96760.7 |
| 92204 |
| 87647.3 |
| 83090.7 |
| 78534 |
| 73977.3 |
| 69420.6 |
| 64863.9 |
| 60307.2 |
| <55750.6 |
| No Value |

Figure 48 - CFD Case 5

54

Figure 49 - CFD Case 5

Finally a simulation with a more detailed mesh was set in order to be able to compare in an appropriate way both concepts.

0:Air_Intake_Full_Out1_open.cas : Scalar: Pressure : : STATE 1   ,TIME 0.00000000E+000
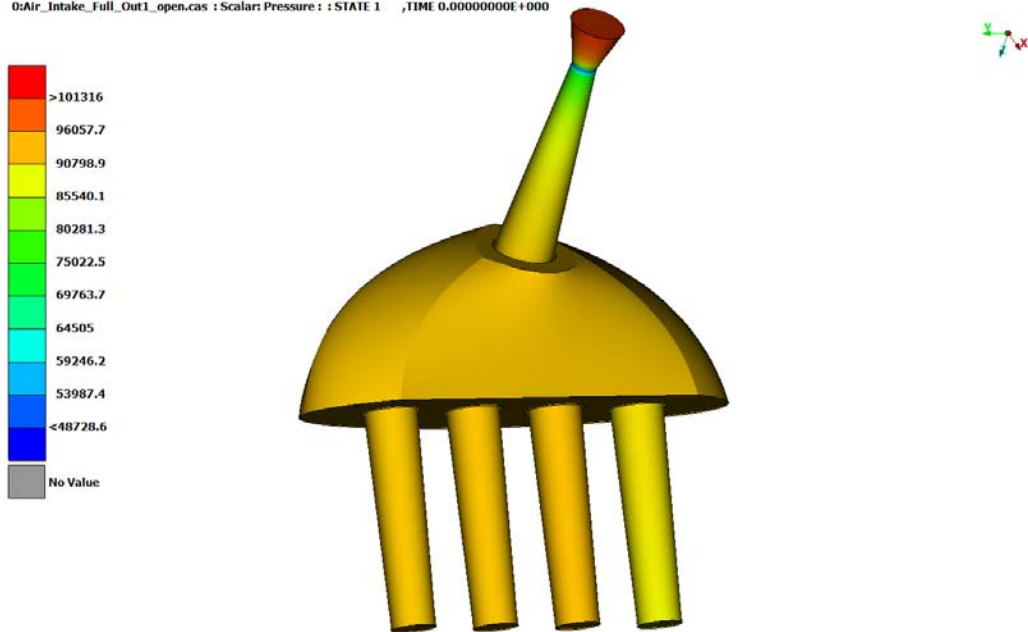

Figure 50 - CFD Case 6

55

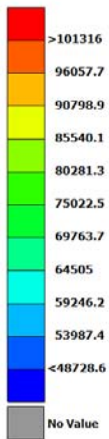0:Air_Intake_Full_Out1_open.cas : Scalar: Pressure : : STATE 1   ,TIME 0.00000000E+000

Figure 51 - CFD Case 6

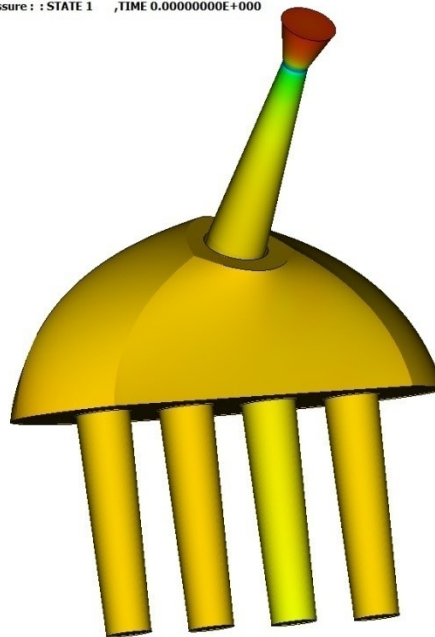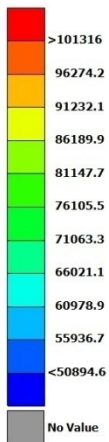0:Air_Intake_VM_medium.cas : Scalar: Pressure : : STATE 1   ,TIME 0.00000000E+000

Figure 52 - CFD Case 6

Institutional Repository - Library & Information Centre - University of Thessaly
05/07/2024 17:39:25 EEST - 3.135.200.17

0:Air_Intake_VM_medium.cas : Scalar: Pressure : : STATE 1   ,TIME 0.00000000E+000

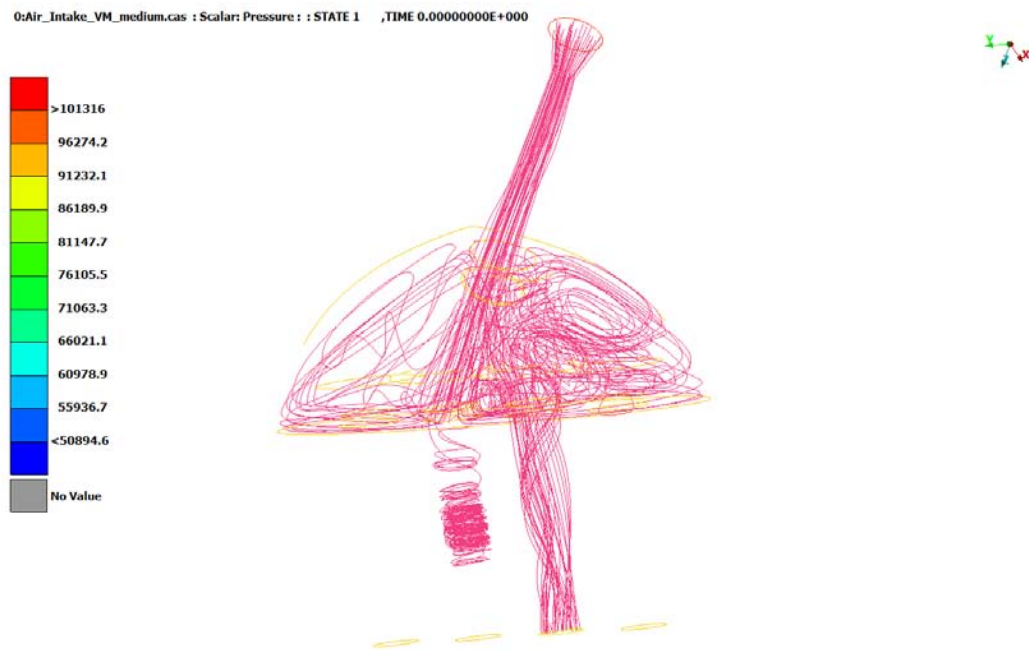|	
	>101316
	96274.2
	91232.1
	86189.9
	81147.7
	76105.5
	71063.3
	66021.1
	60978.9
	55936.7
	<50894.6
	No Value

Figure 53 - CFD Case 6

As can be observed from the above pictures, the results between the two air intake concepts are quite similar with some minor differences. The first observation is related to the quality of grid generation. As already explained, a medium and a finer mesh were implemented for each intake system and the results both for pressure and velocity seem to be almost the same. So it is valid to solve all the possible intake concepts using a less detailed mesh with about 3.000.000 elements and gain significant computational time.

The second observation is related to whether the port is located in the middle or at the outer position of the intake system. Either in the concept with the restrictor cut or in the one with the full restrictor entering the plenum, the middle runners seem to receive more air in contrast with the outer ones, fact that cannot be corrected due to manufacturing restrictions. However, the difference is not considered significant.

Finally, comparing the two concepts the results were found to be similar enough. In designing the plenum, it is important to achieve an even static pressure as this will cause the cylinders to pull the same vacuum, leading to even flow in each cylinder. In order to achieve this goal, a designer is typically faced with a tradeoff: even static pressures are easily achieved by larger plenum volumes, however this not only becomes difficult to package, it affects throttle response as a larger volume increases the amount of time for the system to reach an equilibrium pressure. As can be seen in the pictures below, the pressure distribution inside both systems is even enough. So, the concept with the restrictor cut at the contact patch with the plenum was finally selected because of the less recirculations of air that can be observed, although the differences between the other concept are minor as already stated.
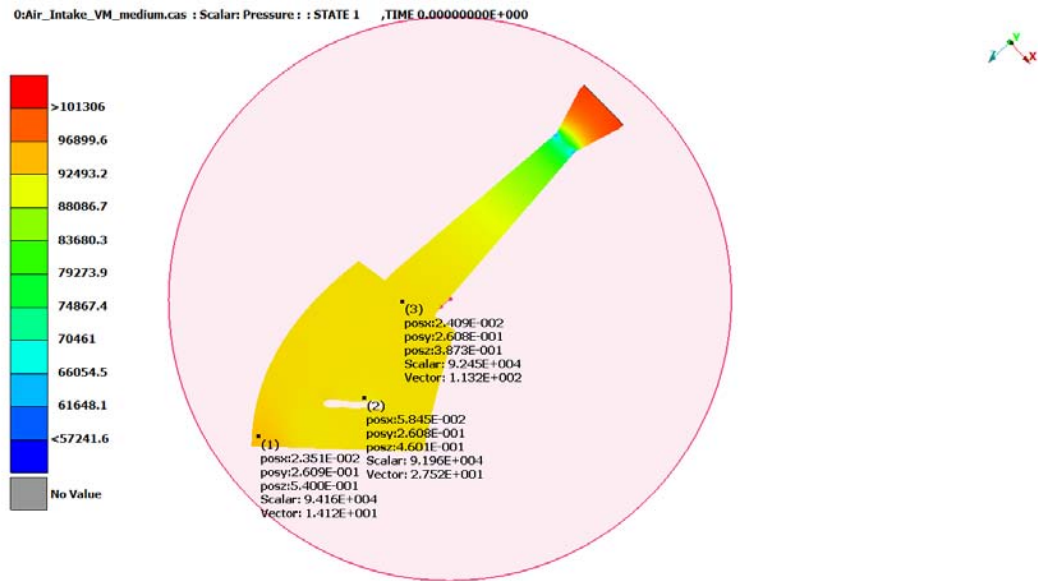
Figure 54- Indicative pressure values for the concept with the restrictor cut
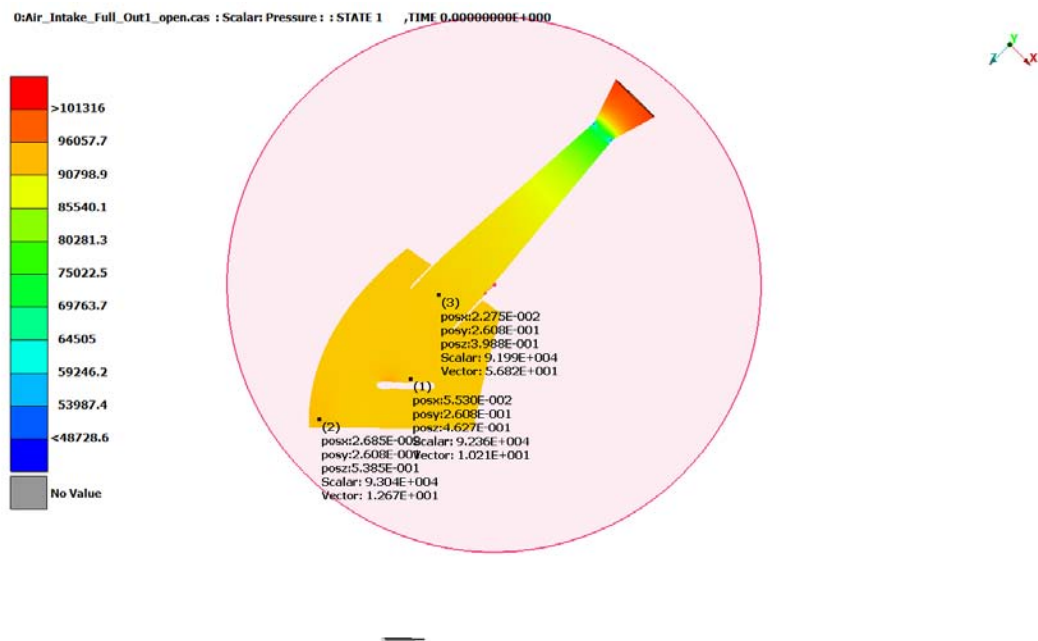

Figure 55 - Indicative pressure values for the concept with the restrictor full

After the final choice the intake system was constructed with the use of aluminum. The restrictor as well as the runners were CNC manufactured and the plenum was constructed with the use of sheet metals.

Afterwards it was implemented on the racecar, Thireus, tested on track and tuned so as to properly function with the rest of the components.

Figure 56 - Thireus competing at Formula Student Germany Competition

Figure 57 - Back view of Thireus featuring the air intake system

6.CONCLUSION AND FUTURE WORK

The scope of this thesis was the design and optimization of an air intake system implemented on a Formula Student single-seat racecar. In order that the final design's formulation would be perfectly understood from the reader, it was considered necessary to explain the general concept of the Formula Student Competition, the parameters that affect an engine's performance as well as the theory behind the Computational Fluid Dynamics procedure.

At first, the basic theoretical background regarding the engine performance was presented, focusing on the needs of a Formula Student engine due to the specific restrictions imposed by the competition. The engine tuning was explained as well as the way the powertrain can be fed with an increased air amount in a specific rpm range without supercharging devices.

Up to next, the parameters of the CFD setup in Ansys fluent were presented and explained in detail in order to show their adequacy for the specific air intake system case. More specifically, the compressibility effect, the turbulence and the boundary layer formation as well as the boundary condition and the kind of solver that was used, were all discussed.

Finally, the whole methodology approach was written from the preliminary considerations regarding the general scopes that the system should follow , until the final CFD setups that were run so as to conclude to the optimum choice.

As a continuation proposal of the current work, it could be considered useful to develop an intake system with the use of carbon fiber or the 3D printing method so as to have the ability to create smoother curves and a more complex geometry and finally achieve a smoother airflow inside the system. Moreover, a system with variable length runners would provide us with the opportunity to take advantage of the ram effect in a wider range of rpms and finally provide the engine with an increased amount of air.

REFERENCES

COMBINED EFFECTS OF VARIABLE INTAKE MANIFOLD LENGTH, VARIABLE VALVE TIMING AND DURATION ON THE PERFORMANCE OF AN INTERNAL COMBUSTION ENGINE ,P Sawant ,Department of Mechanical Engineering and Engineering Science, University of North Carolina at Charlotte, Charlotte, NC 28223-0001, USA , S Bari Department of Mechanical Engineering and Engineering Science, University of North Carolina at Charlotte, Charlotte, NC 28223-0001, USA

OFFICIAL FORMULA STUDENT GERMANY WEBSITE https://www.formulastudent.de/fsg/

DESIGN AND MANUFACTURE OF A FORMULA SAE INTAKE SYSTEM USING FUSED DEPOSITION MODELING AND FIBER-REINFORCED COMPOSITE MATERIALS, Ryan Ilardo, Christopher B. Williams Design, Research, and Education for Additive Manufacturing Systems Laboratory Department of Mechanical Engineering Virginia Polytechnic Institute and State University

Design and manufacture of a Formula SAE Variable Intake Manifold , Juliano Vaz, Allan R. Machado, Rodrigo K. Martinuzzi, Mario E. S. Martins ,Federal University of Santa Maria-Brazil

Formula Student Rules 2020 https://www.imeche.org/docs/default-source/1-oscar/formula-student/fs2020/rules/formulastudentrules2020.pdf?sfvrsn=2

ANSYS FLUENT 12.0 Theory Guide

Wall y+ Strategy for Dealing with Wall-bounded Turbulent Flows , Salim .M. Salim, and S.C. Cheah, Proceedings of the International Multi Conference of Engineers and Computer Scientists 2009 Vol IIIMECS 2009, March 18 - 20, 2009, Hong Kong

INTRODUCTORY LECTURES on TURBULENCE, Physics, Mathematics and ModelingJ. M. McDonoughDepartments of Mechanical Engineering and MathematicsUniversity of Kentucky

Wikipedia https://en.wikipedia.org/wiki/Law_of_the_wall